Chemistry Department

Development of Chitosan and Poly (Vinyl Alcohol) Blended Scaffolds for Cell Culture using Supercritical Fluids Technology

Lígia Marina Clemente Silva

Dissertação apresentada na Faculdade de Ciências e Tecnologia da Universidade Nova de Lisboa para obtenção do grau de Mestre em Mestrado Integrado em Engenharia Química e Bioquímica

Orientador: Professora Doutora Ana Aguiar Ricardo

Monte de Caparica, 2008

In the memory of my dear grandmother Piedade Rosa Lopes

Acknowledgements

The accomplishment of this thesis was only possible due to the contribution of several people, to whom I want to thank.

First of all I would like to express my gratitude to my supervisor Professor Dr. Ana Aguiar Ricardo for hosting me in her lab and for all the help, orientation and transmitted knowledge during these months of work. It was very good to be a part of professor team and to learn about research and the supercritical world.

To Márcio Temtem I want to give a very special thank. He was my advisor, colleague and friend inside and outside the lab and taught me numerous important things. Thank you for the endless help and patience!

The collaboration with Professor Dr. Cláudia Lobato and Pedro Andrade from Instituto Superior Técnico (IST) was fundamental in the work with cells and very important for future work development. Thank you very much!

I also want to thank to all the people that helped me and supplied the necessary equipment to perform this work: Professor Dr. João Sotomayor with contact angles, Professor Dr. Isabel Fonseca with mercury porosimeter, Professor Dr. Helena Godinho and Dr. Pedro Almeida with Dynamic Mechanical Analysis (DMA), Isabel Nogueira (IST) with Scanning Electron Microscopy (SEM), Joana Pais and Mariana Costa with freeze-dryer and Mrs. Conceição and Mrs. Idalina with lab materials.

In the lab there were some other people that helped me along these months, in particular Teresa Casimiro and Mara Silva that were always there to listen and share their experience with high pressure and beyond (I hope to meet the incoming little baby); Eva Vão ("Evita"), João Fernandes ("Évora"), Ricardo Couto ("barbudo"), Silvia Mihaila ("romena") and Eunice Costa ("bio") for all the help and for the funny moments; Also, Telma Barroso ("ti Té") that was my companion in the lab work and in the hard job of writing this thesis in English and for everything else, for the friendship! I am sincerely grateful to all!

A last and singular acknowledgement to my family and friends, particularly, my parents and sister that always support me.

To everyone else that I did not mentioned, but that in some way helped me to get here.

Muito obrigada!

Resumo

Neste trabalho desenvolveram-se novos materiais porosos para aplicações biomédicas utilizando tecnologia supercritica. Neste contexto, preparam-se dois tipos de materiais constituídos por quitosano e álcool polivinílico (PVA) em diferentes proporções: membranas e matrizes tri-dimensionais (3D). As membranas foram preparadas utilizando o método de inversão de fases e usando como não-solvente o dióxido de carbono supercrítico ($scCO_2$). Os resultados obtidos na caracterização destes materiais revelaram que a presença de PVA nas membranas provoca a diminuição da porosidade e do ângulo de contacto e o aumento na interconectividade entre os poros e na capacidade de inchar. As propriedades mecânicas também se alteraram devido à presença de PVA nas membranas, aumentando a capacidade de elongamento e fazendo diminuir o valor da máxima tensão suportada. As matrizes 3D foram preparadas por liofilização e foram reticuladas com glutaraldeído, utilizando uma técnica assistida por CO_2. A optimização deste processo de reticulação envolveu o estudo de diferentes concentrações de glutaraldeído e diferentes tempos de operação. A caracterização morfológica revelou que as diferentes concentrações da solução de polímero estudadas não afectaram a porosidade nem a interconectividade entre os poros das matrizes 3D. No entanto, a presença de PVA na composição destas matrizes e a temperatura utilizada no congelamento das soluções durante a formação das estruturas afectaram a sua morfologia. Estas matrizes porosas demostraram ainda a capacidade de inchar ou contrair quando colocadas em meios com diferentes valores de pH. As matrizes 3D reticuladas com 1% (v/v) de glutaraldeído durante 10 minutos apresentaram os melhores resultados. As membranas e as matrizes 3D foram também submetidas a testes de biodegradabilidade *in vitro* na presença de lisozima e a testes de citotoxicidade, mostrando ser potencialmente aplicáveis em engenharia de tecidos e em medicina regenerativa.

Abstract

In this work new porous materials for biomedical applications were developed using supercritical fluids (SCF) technology. In this context, two types of porous structures constituted by blends of chitosan and poly (vinyl alcohol) (PVA) using different ratios were prepared: membranes and three dimensional (3D) scaffolds. Phase inversion method using supercritical carbon dioxide ($scCO_2$) as non-solvent was used to prepare porous membranes. The characterization of these materials showed that the presence of PVA in the membranes composition causes a decrease in porosity values and contact angle and an increase on pores interconnectivity and swelling degree. The mechanical properties were also modified by the existence of PVA in the membranes composition, increasing the elongation capacity of these structures and decreasing the supported break stresses. The 3D-scaffolds were prepared using freeze-drying technique and were treated with glutaraldehyde using a CO_2-assisted crosslinking process. The optimization of the crosslinking process comprised the study of different glutaraldehyde concentrations and operation time. Morphological characterization showed that the casting solution concentration was a parameter with no influence in the 3D-scaffolds porosity neither on the pores interconnectivity. However, the PVA content in these matrices and the temperature used in the freeze-drying process determined their morphology. These highly porous structures were also submitted to dynamic swelling tests proving to be pH-sensitive with the capacity of swelling and deswelling when submitted to pH variations. The best response was obtained for scaffolds crosslinked with 1% (v/v) of glutaraldehyde during 10 minutes. Membranes and 3D-scaffolds were also tested for *in vitro* biodegradation using lysozyme and for cytotoxicity, proving to have potential applications in tissue engineering and regenerative medicine.

List of Symbols

3D – Three-dimensional

CHT – Chitosan

DMA - Dynamic mechanical analysis

DSC - Differential Scanning Calorimetry

E – Young's modulus

FBS - Fetal Bovine Serum

SCF – Supercritical Fluid

PBS - Phosphate Buffered Saline

*P*c – Critical Pressure

PVA – Poly (vinyl alcohol)

RPMI - Roswell Park Memorial Institute medium

$scCO_2$ – Supercritical carbon dioxide

SEM - Scanning Electron Microscopy

T - Temperature

*T*c – Critical Temperature

Table of contents

Index of Figures

Chapter I

Chapter II

Index of Tables

Chapter I

Chapter II

I. Introduction

1. Supercritical Carbon Dioxide

A Supercritical Fluid (SCF) is defined as a substance above its critical pressure (*P*c) and temperature (*T*c), where the density of the gas phase becomes equal to the density of the liquid phase and the interface between liquid and gas disappears[1] (Figure 1.1).

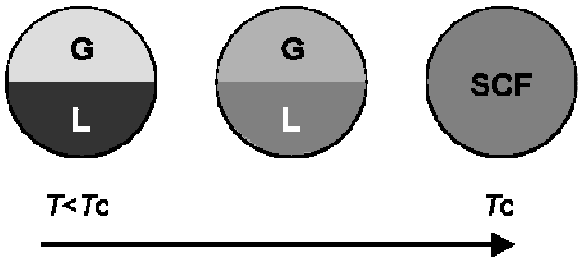

Figure 1.1 - Schematic representation of the change from liquid-gas equilibrium (*T*<*T*c) to supercritical fluid (*T*>*T*c) conditions as a substance is heated above its critical temperature and pressure (adapted from Cooper et al. [2]).

SCFs combine the properties of the two phases, presenting gas-like diffusivity and viscosity and liquid-like density as shown in Table 1.1. In addition, SCFs are highly compressible and their density, and therefore the solvent properties, can be tuned over a considerable range by varying the pressure.[3] Figure 1.2 shows the rapid and continuous increasing in density for pure CO_2 near the *P*c and for a temperature above *T*c.[2]

Table 1.1 – Comparison of typical physical properties of gases, SCFs and liquids

Properties	Gas	SCF	Liquid
Density (kg/m^3)	1	100-800	1000
Viscosity (cP)	0.01	0.05-0.1	0.5-1
Diffusivity (m^2/s)	1.10^{-5}	1.10^{-7}	1.10^{-9}

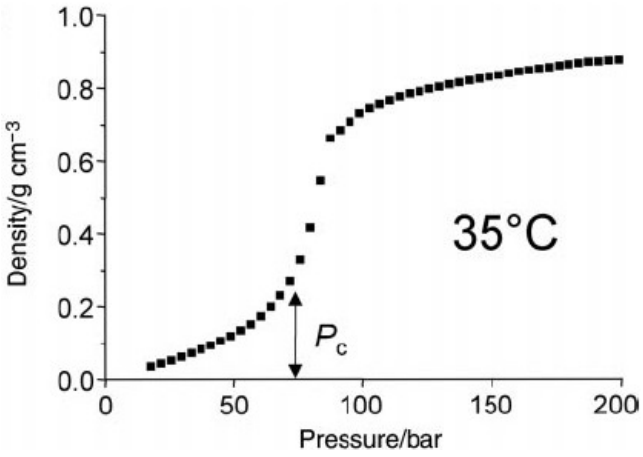

Figure 1.2 - Variation of density with pressure for pure CO_2 at 35ºC. At this temperature (i.e., above *T*c for CO_2) there is a rapid but continuous increase in density near the critical pressure (*P*c) (adapted from Cooper et al.[2]).

The SCF technology involves high pressures and sometimes high temperatures (Table 1.2) and most of the times it will be easier to carry out the experiments under conventional conditions. Even so, there are several advantages when using these fluids for a variety of applications.[4]

Table 1.2 – Critical conditions of a few substances

Substance	*T*c (ºC)	*P*c (MPa)
Carbon dioxide	31.1	7.38
Water	374.2	22.1
Methanol	239.9	8.08
Ethane	31.9	4.87
Propane	96.7	4.25
Toluene	318.6	41.1
Ammonia	132.5	11.3

Supercritical carbon dioxide ($scCO_2$) is the most used SCF because it is an environmentally benign solvent, non-toxic, non-flammable, low cost and readily available in high purity from several sources. Besides, it has an accessible critical point with a *T*c of 31.1 °C and a *P*c of 7.38 MPa (Figure 1.3).

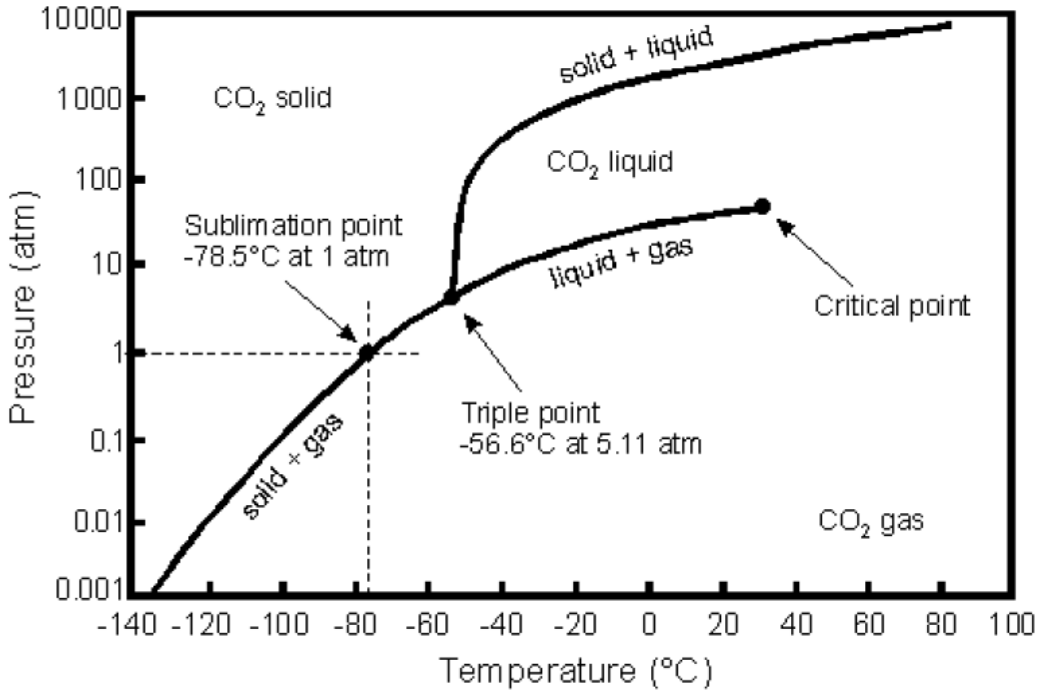

Figure 1.3 – Pressure-temperature phase diagram of pure CO_2 and representation of critical point (*T*c = 31.1 ºC and *P*c = 7.38 MPa).

In recent years, $scCO_2$ has been widely used as a solvent, anti-solvent and plasticizer for synthesis, modification and purification of both synthetic and natural polymers. Therefore, the solvent properties of $scCO_2$, i.e. the solubility of polymers in $scCO_2$ and the solubility of $scCO_2$ in polymers, are very important parameters.[5]

$ScCO_2$ is a very poor solvent for most polymers and pharmaceutical compounds and the polarity of polymers can be a reason for their limited solubility. In addition, CO_2 has the potential to act as both a weak Lewis acid and Lewis base, and theoretical and experimental evidence indicates that CO_2 can participate in hydrogen-bonding interactions. This suggests

that CO_2 might solubilise dipolar and non-dipolar molecular systems through site-specific solute-solvent interactions.[6] Beckman et al.[7,8] have shown that by careful molecular design and choice of co-monomers to balance the solvent–solute and solute–solute interactions it is possible to prepare hydrocarbon based copolymers that are CO_2-soluble. Furthermore, CO_2 solubility and diffusivity in polymers are influenced by both the molecular structure (the interaction between CO_2 and molecular chains) and the morphology (crystalline or amorphous, related with free volume) of polymers.[5]

2. Supercritical Fluids based methods for porous structures production

Porous structures can be prepared using different methods by means of SCF technology like gas foaming[9], supercritical fluid emulsion templating[10] and phase inversion.[11,12,13]

2.1. Gas foaming

The formation of polymer foams occurs when a polymer, plasticized by saturation in the supercritical fluid is rapidly depressurized at a constant temperature. Pockets of gas nucleate and grow in the polymer as the pressure is released and as the supercritical fluid leaves the polymer, the glass transition temperature (*T*g) increases. At the point where the *T*g for the polymer is higher than the foaming temperature, the porous structure is set.[5]

Mooney et al.[14] prepared highly porous matrices from poly (lactic-*co*-glycolic acid) (PLGA) using gas foaming method. However, the scaffolds surface was formed by a non-porous film, making them unsuitable for cell ingress, and presenting a barrier for cell nutrients and for waste products of cell metabolism. This may happen due to the rapid diffusion of the CO_2 from the surface of the scaffold as the pressure is released. Furthermore, it was found that the scaffolds produced had a relatively closed pore-network. To overcome this issue, an additional porogen (sodium chloride crystals of a defined size range) was incorporated into compression moulded PLGA discs before gas foaming. Upon production of the polymer

foam, the porogen was leached out by incubation in water for 48 hours. This created a scaffold with an interconnected pore network open to the surface, which was shown to be accessible to cultured smooth muscle cells. Interconnectivity of the pores could be improved even further by partially fusing the salt porogen by exposure to 95% humidity.[15]

The leaching of the porogen is a major disadvantage of the gas foaming/particulate leaching process since it results in the loss of the majority of any incorporated growth factor. This can be overcome somewhat by encapsulating the active factors in alginate beads which are then incorporated into the compressed polymer together with the porogen before processing. In addition to the issues surrounding salt leaching, the gas foaming process suffers from relatively long manufacturing time.[16]

Under supercritical conditions, CO_2 foams polymers to create porous scaffolds suitable for tissue engineering applications. Since increasing pressure, increases the rate of gas diffusion into polymer systems, equilibration time is reduced compared to subcritical pressures.[17] Gas saturation equilibration times as low as 10 minutes have been reported.[18,19] The effectiveness of this technique in foaming PLGA and use of the scaffolds for tissue engineering has been demonstrated both *in vitro* and *in vivo.*[20,21,22]

Barry et al.[23] used $scCO_2$ to foam the non-degradable polymer poly(ethylmethacrylate)/ tetrahydrofurfuryl methacrylate (PEMA/THFMA), which has been shown to be an excellent scaffold material for cartilage repair. It was verified the formation of a surface skin, however a greater degree of pore interconnectivity (up to 57%) was found compared to that reported for the gas foaming technique applied to PLGA. *In vitro* cell culture revealed enhanced phenotypic maintenance of chondrocytes cultured on the foamed material (as measured by extracellular matrix secretion), demonstrating the utility of a three-dimensional environment for promoting tissue regeneration. Further optimisation of the processing conditions of PEMA/THFMA demonstrated that the degree of porosity and their interconnectivity could be tightly controlled simply by controlling the venting rate. In this process, an additional

porogen/leaching process is not necessary. As might be expected, as porosity increases, mechanical strength decreases and this is an important factor in many biomedical applications. There is therefore an upper limit, above which pore size and low mechanical strength precludes their use in certain applications.[24]

In attempting to improve the mechanical properties of the THFMA for soft prosthetic applications, the foaming of blends of THFMA with styrene–isoprene–styrene copolymer elastomer has been investigated. Mechanical testing revealed the blends to be elastomeric, and these systems may therefore lend themselves to use as scaffolds for particular tissues, such as cartilage. The degree of porosity and interconnectivity of the pores could be tuned by modifying the blend composition and processing temperature, with a reduction in the degree of foaming as temperature increased.[25]

Similarly, Mathieu et al.[18] have shown that the morphology of the foams can be controlled to mimic the bone structure. They found that by controlling the cooling rate of the foamed polymer and the density of the gas nucleation similar bone structures could be formed. Rapid cooling creates many spherical pores while slower cooling permits pores elongation. Alternatively, the interconnectivity of the pores can be improved by post-processing the scaffolds generated by gas foaming using ultrasound. Wang et al.[26] produced polymer foams of poly(lactic acid) (PLA) (using sub-critical pressures of CO_2) and exposed them to pulsed ultrasound at a frequency of 20 kHz and average power input of 100 W. This not only slightly increased pore size, but also improved their interconnectivity as a result of pore wall rupture.

2.2. Supercritical fluid emulsion templating

An alternative to the use of supercritical fluids in the gas foaming of polymers to create porous scaffolds is emulsion templating. Here, a variety of porous hydrophilic materials can be produced by reaction-induced phase separation of concentrated oil-in-water emulsions. Conventional methods require large amounts of water immiscible organic phases as the

internal phase (usually > 75%), which can be difficult to remove after the reaction. For example, for inorganic materials temperatures > 600°C are often used, which would clearly not be appropriate for thermolabile materials or those containing growth factors for regenerative medicine.

Butler et al.[27] demonstrated that the emulsion templating principle can be applied to supercritical CO_2-in-water (C/W) emulsions. Using perfluoropolyether (PFPE) surfactants and PVA to stabilize the C/W emulsions of acrylamide polymers, they vented the CO_2 following polymerization, leaving polymer scaffolds with interconnected pores (Figure 1.4). Increasing the volume fraction of the CO_2 internal phase increased porosity, and increasing the surfactant concentration led to more open interconnected structures.

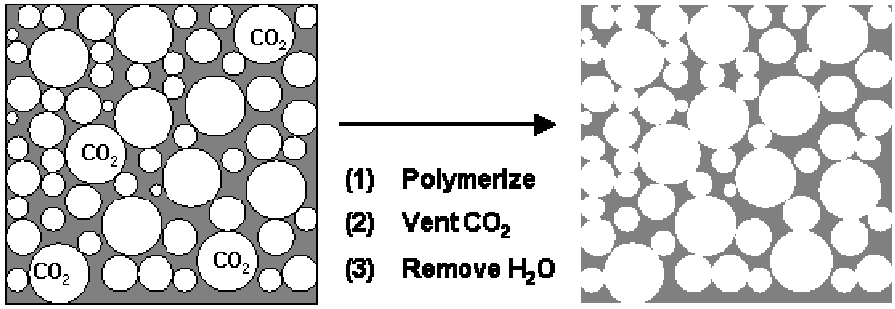

Figure 1.4 - Schematic of the preparation of porous materials using supercritical fluid emulsion templating. The external phase is an aqueous solution and the internal droplet phase is $scCO_2$ (adapted from Butler et al. [10]).

A disadvantage of this protocol for bioengineering applications is the use of a non-degradable surfactant, and the mean pore sizes (~50 μm) produced may not be suitable for all applications — it has been reported that scaffolds for bone regeneration for example require pore sizes between 200 and 400 μm.[28]

A variation on the emulsion templating technique has recently been reported by Partap et al.[29], who produced emulsion templated alginate hydrogels in which the $scCO_2$ not only served as the templating "oil" phase, but also as a source of acidity used to release Ca^{2+} from

its chelated form, freeing it to crosslink the alginate and form the porous hydrogel. Calling the technique "reactive emulsion templating", they were able to produce 3D hydrogels with an open and interconnected porous network, with a mean pore size similar to the emulsion templating technique reported by Butler et al.[10].

2.4. Phase inversion

The majority of porous membranes are prepared from a homogenous polymer solution by the wet phase inversion method. In this method, a homogeneous polymer solution is loaded on a support and immersed in a coagulation bath containing a non-solvent. The formation of the porous structure occurs due to the exchange of solvent and non-solvent that causes a decrease in solvent power and the polymer precipitates. So, the affinity between solvent and non-solvent, as well as polymer concentration, temperature, humidity, evaporation time and composition of the casting solution are very important parameters that allow the control of membrane morphology.[11,12,13]

One of the main concerns when using this method is that some solvents are volatile, flammable and may cause risk to health and environment. For this reason and due to the presence of residual solvents that can cause potential problems in biomedical applications, membranes are normally submitted to intensive post-treatments. Moreover, long formation times and a limited possibility to modulate cell size and membrane structure characterize this process.

Kho et al.[30] used a new technique in which $scCO_2$ is used to induce the phase separation of the polymer solution. Compared with the wet phase inversion method, advantages of this phase separation process can be:

(1) $ScCO_2$ can dry the polymer membrane rapidly and totally without the collapse of the structure due to the absence of a liquid–vapour interface. The dry membrane can be obtained without additional post-treatment because there are no traces of organic solvents.

(2) It is easy to recover the solvent; the solvent dissolved in $scCO_2$ can be removed from gaseous CO_2 in a separator located downstream the membrane formation vessel.

(3) CO_2 is not toxic, not flammable and low cost.

Kho et al. used compressed CO_2 for the formation of Nylon 6 membranes. A 15% (w/w) Nylon 6 polymer solution was prepared by dissolving Nylon 6 in 2,2,2-trifluoroethanol. Thin film with thickness ranging from 150 to 250 μm was obtained. The process was performed at 35ºC with the final pressure up to 17.4 MPa, for 30 minutes. These authors obtained uniform structures with cellular pores 0.4 μm in diameter. They described the structural gradient and pore characteristics of the membranes by a competition between a liquid–liquid (L–L) demixing, that originates soft cellular pores and solid–liquid (S–L) demixing, that originates rough structures. The authors concluded that reducing the relative strengths of both the solvent and the non-solvent, led to membrane pore structures dominated by crystallization (S–L demixing), that is the thermodynamically favoured demixing process, rather than L–L demixing, which is kinetically favoured.

Another membranes formation process, in which $scCO_2$ is used as non-solvent, has been presented by Matsuyama et al.[31]. The process consists of the introduction of CO_2 into a membrane formation cell through a buffer tank using a valve that connects the two vessels. After the system has been equilibrated (for 15 minutes) at the pressure of 130 bar, a second valve is opened and CO_2 flows in the cell to dry the phase-separated polymer solution. Matsuyama et al. studied the formation of thin polystyrene membranes analysing the effect of several process conditions (temperature, pressure, polymer concentration). They observed that the average pore size ranged from 8 to 35μm changing pressure (from 75 to 150 bar), polymer concentration (from 15 to 30% (w/w)) and temperature (from 20 to 70ºC).

In a successive work, Matsuyama et al.[32] studied the influence of different solvents used during the formation of cellulose acetate membranes. The authors worked with all fixed process parameters: pressure, temperature and polymer concentration (130 bar, 35ºC, 15%

(w/w)) and tested four solvents: acetone, methyl acetate, 1,3-dioxolane and 2-butanone. They noted that, as the mutual affinity between the solvent and CO_2 decreases, the membrane porosity and the pores size increases.

Using the $scCO_2$ assisted phase inversion method, Reverchon and Cardea[13] studied the formation of cellulose acetate membranes from acetone, polysulfone membranes from N-methylpyrrolidone and chloroform, poly-L-lactide membranes from chloroform, and poly(methyl methacrylate) membranes from dimethylsulfoxide, acetone, and tetrahydrofuran. The overall result of these studies is that, changing the supercritical based process parameters, it is possible to modulate cell and pore size and to obtain various morphologies using the same liquid solvent: cellular structure, binodal structure, and microparticles. In some cases, it is also possible to modulate all membrane characteristics simply changing the non-solvent power of $scCO_2$.

Temtem et al. [11] studied the solvent affinity and depressurization rate on the morphology of polysulfone (PS) membranes produced by CO_2-assisted phase inversion method, of six different organic solvents and two depressurization rates. This study showed that mutual affinity between solvent and non-solvent and the depressurization rate influence the membranes morphology when $scCO_2$ is used as non-solvent. They also studied the preparation of membranes with polysulfone/polycaprolactone (PS/PCL) blends using a CO_2-assisted phase inversion method.[12] The CO_2 capability to swell PCL and decrease the *T*m was used to produce and control the porosity and the properties of the membranes. In this study it was shown that CO_2-assisted phase inversion method combined with the capability of CO_2 to act as a blowing agent can be used to produce PS/PCL membranes. By adjusting the PS/PCL ratio it was possible to vary the morphology, the hydrophilicity and the mechanical performance of the membranes. This was the first attempt to combine CO_2 foaming ability with phase inversion process for membranes production with polymer blends.

In conclusion the use of $scCO_2$ as a non-solvent allows the preparation of sterile and ready to use devices, since CO_2 is a gas under ambient conditions and can be easily removed from the polymeric product without leaving residues and, consequently, without requiring additional post-treatments.[5] Moreover, it is possible to recover the solvent from CO_2 during depressurization, mass transfer is improved (much lower viscosities than organic liquids, and easily adjusted with variations in pressure and temperature) and there is a better control of membranes morphology, due to the introduction of more parameters (pressure, CO_2 flow, depressurization rate).[11]

Even so, $scCO_2$ has a low affinity to some solvents, namely water, at the ordinary process conditions (40-60ºC, 100-250 bar) being unable to produce membranes of water soluble polymers. The alternative is to use a co-solvent (ethanol, for instance) in addition to $scCO_2$ flow to increase the solubility of the solvent in CO_2[33]. The ratio of the co-solvent will also influence the membrane morphology and, as the other parameters, must be controlled in order to obtain porous structures with the desired morphology.[34]

Figure 1.5 represents an isothermal phase diagram for the system polymer-solvent-non-solvent ($scCO_2$) at pressures above the critical point of the binary mixture solvent+CO_2. As explained above, the affinity between solvent and non-solvent, as well as polymer and solvent are some of the parameters that must be controlled to obtain the desired membrane morphology. All possible composition combinations of the components can be plotted in this diagram, where the corners represent each intervenient: i) the polymer; ii) the solvent and iii) the non-solvent – ($scCO_2$). The type of structures obtained and the pore dimensions are related with the thermodynamics and kinetics of the phase-inversion process, depending on the path through the ternary diagram.[35,36]

The diagram presents a liquid-fluid region where the spinodal and binodal curves enclose demixing boundary. The point where the binodal and the spinodal coincide is the critical point and the region between the curves corresponds to a metastable state.

Nucleation and growth (usually a slow process) is the expected mechanism when a system leaves the thermodynamically stable condition and slowly enters the metastable region and can be represented in the ternary diagrams by the two distinguish paths: Path (4) – demixing starts somewhere below the critical point – nucleation and growth of the polymer-rich phase occurs and microparticles are obtained. Path (2) – demixing starts somewhere above the critical point - nucleation and growth of the polymer-poor phase occurs with further solidification of the polymer-rich phase which forms a membrane cellular structure.

Another mechanism is spinodal decomposition that occurs in a transition that crosses the metastable region near the critical point. Path (3) - demixing starts with concentration fluctuations of increasing amplitude, giving rise to two continuous phases, forming a bicontinuous (spinodal) membrane structure.

Finally, Path (1) – demixing occurs when the outflow of the solvent from the solution is faster than the inflow of the non-solvent and the polymer molecules solidifies by gelation or crystallization into a dense structure.

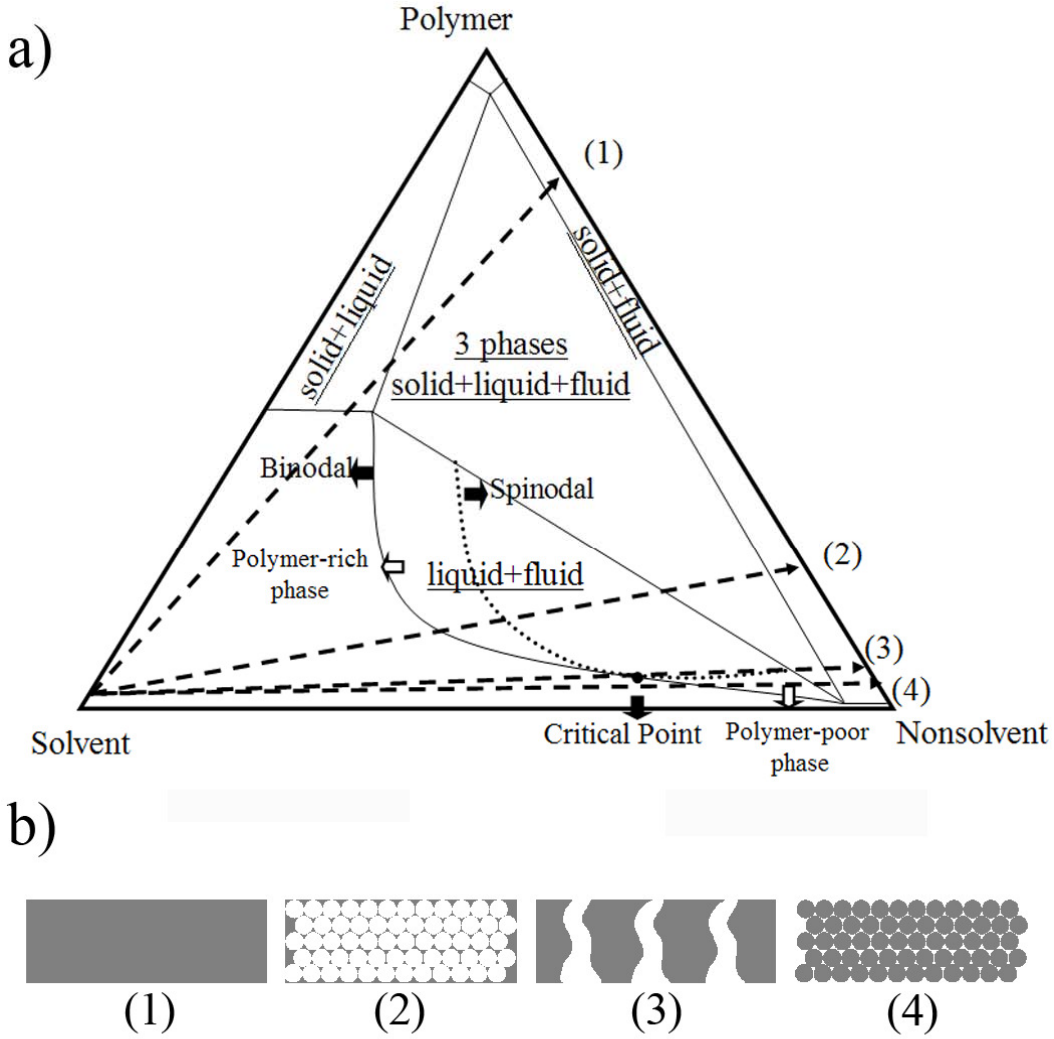

Figure 1.5 – a) Schematic representation of an isothermal phase diagram for the system polymer-solvent-non-solvent at pressures above the critical point of the binary mixture solvent+CO_2; b) obtained structures at different composition paths: (1) dense structure, (2) cellular morphology, (3) bicontinuous morphology and (4) microparticles (adapted from Temtem et al. [34]).

3. Freeze-drying method

Besides SCF based techniques to prepare porous structures other conventional methods have been studied, including fiber bonding, particulate leaching, melt molding and emulsion freeze-drying.[37]

In emulsion freeze-drying, an emulsion is prepared by homogenization of a polymer–solvent system. The continuous phase consists of the polymer-rich phase, while solvent is the dispersed phase. The emulsion is cooled down quickly to freeze the solvent and water by immersion in a freezing bath (for example, liquid nitrogen). This results in solidification of the polymer directly from the liquid state and the creation of porous polymer structure. Subsequently, the frozen solvent is removed by lyophilization[38] (Figure 1.6).

Several parameters must be controlled such as casting solution composition and freezing temperature to obtain the desirable pores morphology.[39] This method has been used to fabricate aliphatic polyester-based scaffolds by Whang et al.[40,41]. Scaffolds with porosities higher than 90%, median pore sizes ranging from 15 to 35 μm with larger pores greater than 200 μm were prepared. The scaffold pore architecture was highly interconnected what is essential for tissue ingrowths and regeneration.

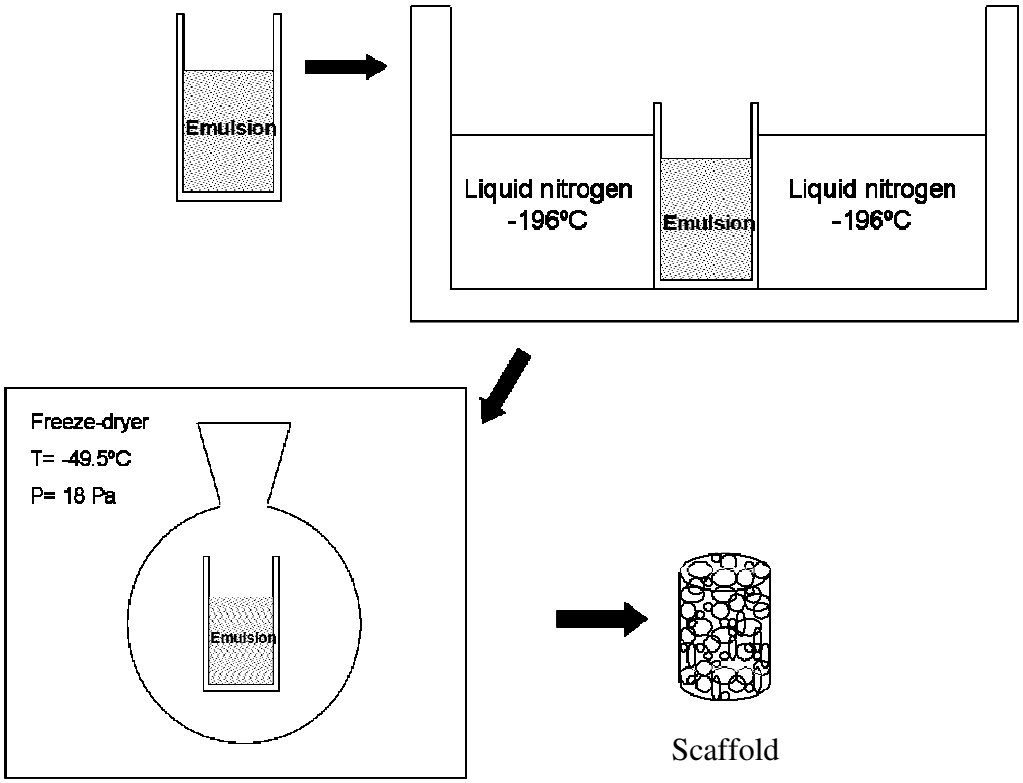

Figure 1.6 – Schematic representation of emulsion freeze-drying process (adapted from Whang et al.[40]).

This technique has been devised for incorporating proteins into the polymer scaffolds. Freeze-drying of aqueous solutions of natural biopolymers such as collagen has been reported for the production of well defined porous matrices (i.e., pore size and orientation) based on the controlled growth of ice crystals during the freeze-drying process.[37,42] Also, chitosan has been used as a structural base material for scaffolds production using freeze-drying process. Scaffolds with specific shapes and size and with control over pore morphology were prepared by Madihally et al.[43]

However, the emulsion freeze-drying method is user and technique sensitive. The fabrication of a truly interconnecting pore structure depends on the processing method and parameters as well as on the used equipment.[44,45]

4. Crosslinking process

To enhance biostability and mechanical properties, scaffolds can be submitted to a physical or chemical crosslinking treatment. Physical processes consist in UV radiation, freeze-drying or heating; while in chemical processes it can be used ionic crosslinking or chemical crosslinkers such as glutaraldehyde and carbodiimide[46].

There are different crosslinking procedures described in literature. For example, PVA can be physically crosslinked by repeated freeze-thawing cycles of aqueous polymer solutions or chemically crosslinked with glutaraldehyde (Figure 1.7 (b)), succinyl chloride, adipoyl chloride and sebacoyl chloride. It can also be blended with other water-soluble polymer and again crosslinked either physically or chemically. Chitosan derivatives and blends have been chemically crosslinked using glutaraldehyde (Figure 1.7 (a)), epichlorohydrin or ethylene glycol glycidyl ether and physically crosslinked by UV radiation and thermal variations.[47,48]

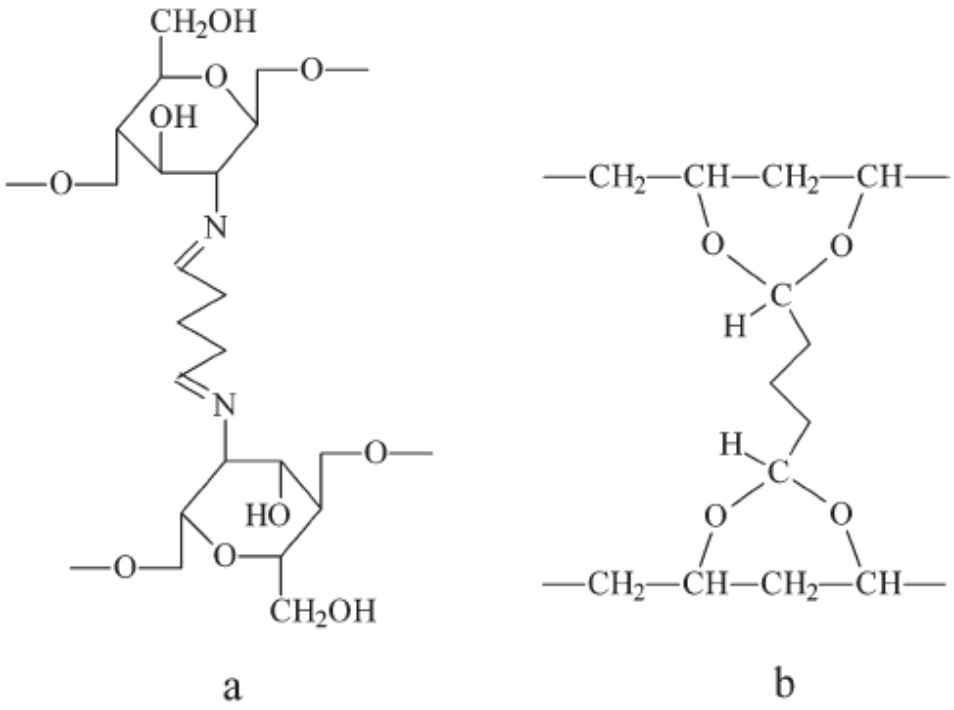

Figure 1.7 - Schematic representation of (a) chitosan and (b) PVA crosslinked with glutaraldehyde (adapted from Li et al. [48]).

Glutaraldehyde is one of the most used chemical crosslinkers since it is less expensive than other reagents, is readily available and is highly soluble in aqueous solution.

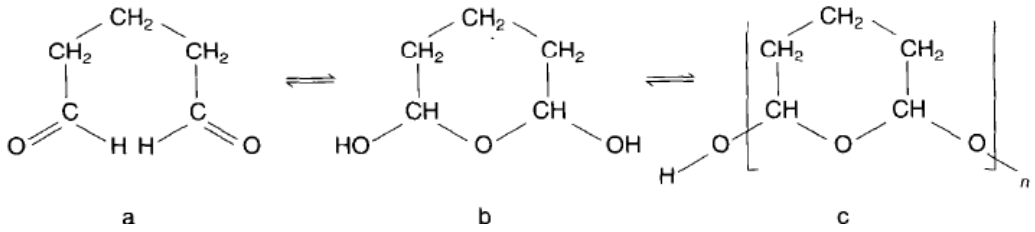

Figure 1.8 – Equilibrium of glutaraldehyde in aquous solution (adapted from Jayakrishnan and Jameela [49]).

There are different crosslinking procedures described in literature to prepare chitosan-based hydrogels and chitosan microspheres or membranes, using glutaraldehyde. Yao et al.[50] reported a procedure for the preparation of semi-interpenetrating hydrogel based on glutaraldehyde crosslinked chitosan with an interpenetrating polyether polymer network.

Gohel et al.[51] reported on chitosan microspheres where glutaraldehyde was used as a crosslinking agent. Thacharodi and Rao[52] studied propranolol hydrochloride delivery systems using various chitosan membranes with different crosslink densities as drug release controlling membranes. The drug release was significantly reduced when crosslinked chitosan membranes were used. Moreover, the drug release rate was found to depend on the crosslink density within the membranes. It was observed that the device constructed with a chitosan membrane with a high crosslink density released the minimum amount of drug. This is due to the decreased permeability coefficient of crosslinked membranes resulting from the crosslink points.

One of the major concerns when using glutaraldehyde is its toxicity, which has lead to several studies. It was concluded that the operation time, concentration of the reagent and temperature were important parameters that should be optimized to reduce or eliminate toxicity due to glutaraldehyde. Also, Ruijgrok and De Wijn[53] showed that not only the amount of reagent but also its nature and distribution are important. The crosslinker should be distributed uniformly throughout the thickness of the material. They showed that high temperature enhances the crosslinking and allows lower concentrations of glutaraldehyde. Thus, by optimizing the time, temperature and concentration of the reagent, it is possible to obtain a more uniform network.[49]

5. Biomaterials in tissue engineering

The search for materials with appropriate physical and chemical properties to apply in biomedical field has lead to intensive investigation.[54,55,56] Ceramics and metals were studied by several researchers, including Ducheyne and Qiu[57], Puleo and Nanci[58] and Rosen et al.,[59] for orthopedic applications. Despite the contribution of these materials to major advances in the medical field, they are not biodegradable and their processability is very limited. Polymer

materials have received increasing attention and been widely used for tissue engineering because of easy control over biodegradability and processability.[54]

Both natural and synthetic polymers have been studied for tissue engineering applications. The naturally derived polymers include proteins of natural extracellular matrices such as collagen and glycosaminoglycan, chitosan and polypeptides.[60] Chitosan, a naturally derived polysaccharide is obtained by alkaline deacetylation of chitin, the principal component of protective cuticles of crustaceans such as crabs, shrimps, lobsters and cell walls of some fungi. Chitosan structure is represented in Figure 8, presenting one primary amino and two free hydroxyl groups for each C6 building unit. Due to the easy availability of free amino groups in chitosan, it carries a positive charge and thus in turn reacts with many negatively charged surfaces/polymers and also undergoes chelation with metal ions (Fukuda[61]). Thus, it is utilized for separation of metals. Chitosan is a weak base and is insoluble in water and organic solvents, however, it is soluble in dilute aqueous acidic solution (pH < 6.5), which can convert the glucosamine units into a soluble form $R–NH_3^+$. It gets precipitated in alkaline solution or with polyanions and forms gel at lower pH. It also acts as flocculant for the treatment of waste water. Properties such as biodegradability, low toxicity and good biocompatibility make it suitable for use in biomedical and pharmaceutical fields, for example it is used in wound[62] and burn healing,[63] in ophthalmology[64] and in the form of membranes that were found useful as artificial kidney membranes because of their suitable permeability and high tensile strength.[65] In spite of the advantages of this polymer there are certain limitations and concerns regarding their use. Lee et al.[66] showed that it is difficult to control mechanical properties and degradation rates of the naturally derived polymers.

Proper characterization and screening of the natural materials lighten many of the concerns, but overcoming the materials limitations is more challenging. Several approaches have been taken to overcome these limitations, including graft polymerization and blending with other natural or synthetic polymers. Polymer blends have shown favourable results in terms of the

targeted biological, mechanical or degradation properties in comparison to the individual components.[54,55,56]

In the case of synthetic polymers, they can be tailored to have a much wider range of mechanical and chemical properties than natural polymers. They also avoid the concern regarding immunogenicity, but Seal et al.[67] demonstrated that biocompatibility becomes a problem. For the purposes of biomaterials, synthetic polymers may be classified as non-degradable and degradable polymers. Non-degradable polymers that are biocompatible and have been used extensively include poly(tetrafluoroethylene) (Teflon) for applications such as vascular grafts[68] and high density polyethylene for use in hip implants,[69] among other applications. While the non-degradable polymers can be fabricated with an extremely wide range of well controlled properties, their permanence does raise concern regarding their long-term effects, especially with regards to wound and inflammatory response.[70]

Thus, there has been a great deal of research into the development of degradable synthetic polymers which would, in theory, have all the properties of their non-degradable counterparts, but also avoid the long-term issues by degrading to metabolizable components.[71]

PVA presents a good alternative to form a blend with chitosan because it is a biodegradable synthetic polymer, innocuous and biocompatible allowing its applications in biomedical field. Additionally it is highly hydrophilic and has an excellent chemical resistance and physical properties.[63] The intermolecular interactions between the two polymers it is also important in the blend formation and morphology. In this case, due to its functional groups, chitosan is potentially miscible with PVA (Figure 1.9).[72]

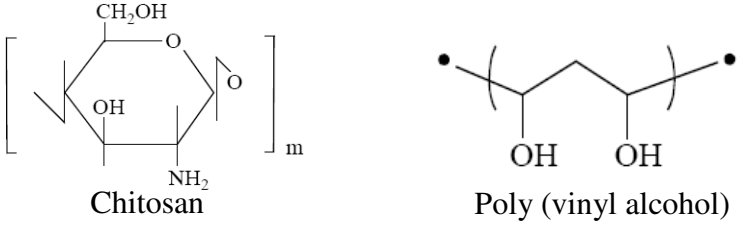

Chitosan Poly (vinyl alcohol)

Figure 1.9 – Structures of chitosan and PVA (adapted from Bahrami et al. [73]).

Chitosan membranes blended with PVA have already been reported to have good mechanical properties because of the specific intermolecular interactions between PVA and chitosan in the blends.[74] Uragami et al.[75] prepared crosslinked PVA/chitosan blend with a fixed amount of crosslinking agent and studied the active transport of halogen ion through the blend membrane. Kim et al.[76] reported the pH sensitive swelling properties of crosslinked PVA/chitosan blend membrane. Chaung et al.[72] reported that the use of PVA/chitosan blend membrane was more favourable for fibroblast cell culture than the single components and best suitable for wound dressing.

Besides membranes, several researchers have also studied chitosan and PVA blended films[77] and hydrogels[78,79] for drug delivery and tissue engineering applications.

In tissue engineering, the intent is to develop supports for tissue repair and regeneration, such as polymer matrices, formed by biocompatible and biodegradable materials.[60] Initially, it was thought that cells might be able to organize into tissues and, ultimately, organ replacements if they were cultured in three dimensions under the appropriate reactor conditions. Refined considerably, this approach remains the foundation of this field. The matrices, also known as "scaffolds", to create the three-dimensional environment have been designed with particular surface chemistries, architectures, and degradation rates to promote and direct cellular attachment, migration, proliferation, and differentiation (Yang et al.,[80] Chen et al.,[60] Nguyen and West[81]). So, the biocompatibility of materials revealed to be of great importance in developing new structures for biomedical applications. There are several general characteristics that need to be considered for all scaffolds designs, although the final requirements depend on their specific purpose. The prepared structures must mimic the native extracellular matrix, an endogenous substance that surrounds cells, attach them into tissues and provide signals that help cellular development and morphogenesis.[38,60] In addition, scaffolds should absorb body fluid for transfer of cell nutrients and metabolites through the

material, which is managed by the pore structure. For this reason, it is very important to create devices with a high porosity and good pore interconnectivity to promote cell adhesion and growth, allowing nutrient delivery, waste removal, protein transport, gaseous exchange and general vascularization.[82] Besides, the mechanical properties of the matrices should match those of the tissue at the implantation site or at least protect the cells from compressive or tensile forces that may damage them. The matrices must be formed by biocompatible and biodegradable materials, bioadsorbed after a determined time period and replaced by grown tissue.[60]

In Figure 1.10 it is represented the principle of tissue engineering: cells are isolated from a donor tissue and cultured on a scaffold *in vitro* and then implanted *in vivo*.[38]

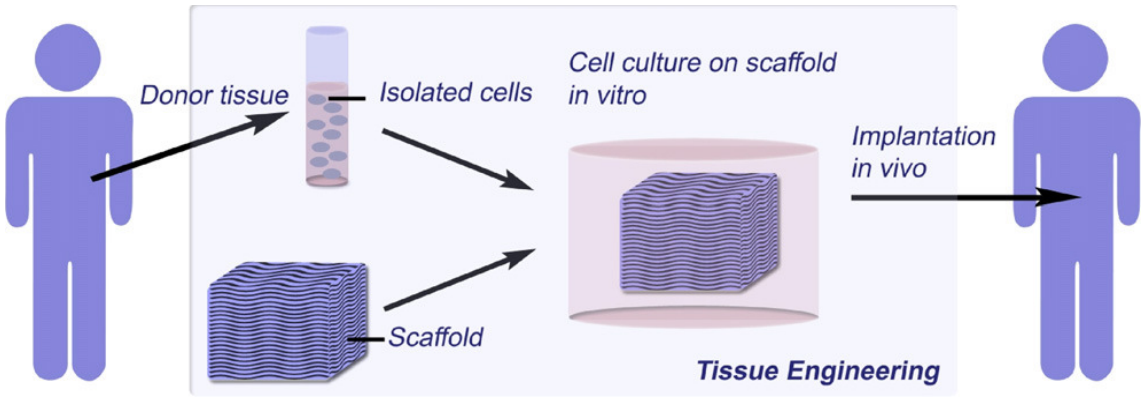

Figure 1.10 - The principle of tissue engineering (adapted from Stamatialis et al. [38]).

So, besides scaffolds, it is also important to study the cells to be implanted. Cell sources for tissue engineering have expanded tremendously, and fully differentiated cells, progenitors, and stem cells have shown great promise for the creation of the highly complex, functional tissues needed to address the tissue and organ loss in medicine (Shamblott et al.;[83] Morrison et al.;[84] Solter and Gearhart;[85] Gage;[86] Boheler et al.;[87] Jackson et al.[88]). However, there are significant issues that must be understood and addressed to realize this potential. In particular, while stem cells and progenitors of various origins have been shown to differentiate into a

variety of cell types and, in some cases, form functional tissues (Levenberg et al.[89]), it remains challenging to differentiate the progenitors and stem cells in a controlled, efficient, and reproducible manner which results in terminally differentiated tissue structures. Tissue engineering may provide a means to gain critical insight into the behaviour of stem cells, by facilitating the control of the stem cell environment both chemically and physically in three dimensions. This, in turn, may lead to the development of new tissue substitutes and replacements.[54]

6. Aim and outline of this thesis

The conventional methods for the production of porous structures are either multi-step processes or needing organic solvents but the production of solvent-free structures is possible by using SCF technology. Although there are numerous examples of porous structures formation with SCF, the $scCO_2$-assisted phase inversion method is one of the most used in membranes production. A method that does not use SCF, but it is applied in the production of 3D-scaffolds highly porous and with good pore interconnectivity, to support cell adhesion and growth, is the freeze-drying method.[82]

The aim of this thesis is to develop chitosan and PVA blended scaffolds with biocompatible and biodegradable properties for biomedical applications by means of SCF technology.

The present chapter gives a general overview of SCF techniques used in scaffolds production, explains the freeze-drying method and presents a summarized description of the crosslinking process. In chapter I, the importance of biomaterials in tissue engineering is also reported.

Chapter II comprises the preparation of chitosan and PVA blended membranes and 3D-scaffolds, their characterization and the evaluation of biodegradable and cytotoxic tests in these porous structures. The $scCO_2$-assisted phase inversion technique was the elected method

to prepare membranes with different PVA ratios to study the influence of the casting solution composition in the structures morphology. The 3D-scaffolds will be prepared using freeze-drying technique and treated by means of $scCO_2$-assisted crosslinking process. The influence of different casting solution compositions and percentages and different freezing temperatures in the scaffolds morphology will be analysed. The crosslinking process will also be an important aspect of this work and it will be studied for different crosslinker percentages and operation times. The characterization of membranes and scaffolds includes the determination of the mechanical properties (dynamic mechanical analysis (DMA)), morphology (scanning electron microscopy (SEM)), porosity (mercury porosimetry), hydrophobicity (contact angles), swelling and *in vitro* biodegradability. Finally, the cytotoxicity of membranes and 3D-scaffolds will be evaluated, following International Standard guidelines, to conclude about the possible use of these devices to sustain stem cell function and proliferation for application in clinical settings.

7. References

[1] F. Cansell, C. Aymonier, A. Loppinet-Serani, Review on materials science and supercritical fluids, Current Opinion in Solid State and Materials Science 7 (2003) 331-340.

[2] A. I. Cooper, Polymer synthesis and processing using supercritical carbon dioxide, J. Mater. Chem., 10 (2000) 207-234.

[3] R. A. Quirk, R. M. France, K. M. Shakesheff, S. M. Howdle, Supercritical fluid technologies and tissue engineering scaffolds, Current Opinion in Solid State and Materials Science, 8 (2004) 313-321.

[4] J. A. Darr, M. Poliakoff, New Directions in Inorganic and Metal-Organic Coordination Chemistry in Supercritical Fluids, Chem. Rev., 99 (1999) 495-541.

[5] O. R. Davies, A. L. Lewis, M. J. Whitaker, H. Tai, K. M. Shakesheff, S. M. Howdle, Applications of supercritical CO_2 in the fabrication of polymer systems for drug delivery and tissue engineering, Advanced Drug Delivery Reviews 60 (2008) 373–387.

[6] P. Raveendran, Y. Ikushima, S. L. Wallen, Polar Attributes of Supercritical Carbon Dioxide; Acc. Chem. Res., 38 (2005) 478-485.

[7] E. J. Beckman, A challenge for green chemistry: designing molecules that readily dissolve in carbon dioxide, Chem. Commun., 17 (2004) 1885-1888.

[8] T. Sarbu, T. Styranec, E. J. Beckman, Non-fluorous polymers with very high solubility in supercritical CO_2 down to low pressures, Nature, 405 (2000) 165-168.

[9] J. J. A. Barry, S. N. Nazhat, F. R. A. J. Rose, A. H. Hainsworth, C. A. Scotchford, S. M. Howdle, Supercritical carbon dioxide foaming of elastomer/heterocyclic methacrylate blends as scaffolds for tissue engineering, J. Mater. Chem., 15 (2005) 4881-4888.

[10] R. Butler, C. M. Davies, I. Hopkinson, A. I. Cooper, Emulsion Templating using Supercritical Fluid Emulsions, Polymer Preprints, 43 (2002) 744-745.

[11] M. Temtem, T. Casimiro, A. Aguiar-Ricardo, Solvent power and depressurization rate effects in the formation of polysulfone membranes with CO_2-assisted phase inversion method, Journal of Membrane Science, 283 (2006) 244-252.

[12] M. Temtem, T. Casimiro, J. F. Mano, A. Aguiar-Ricardo, Preparation of membranes with polysulfone/polycaprolactone blends using a high pressure cell specially designed for a CO_2-assisted phase inversion, J. of Supercritical Fluids, 43 (2008) 542-548.

[13] E. Reverchon, S. Cardea, Formation of cellulose acetate membranes using a supercritical fluid assisted process, Journal of Membrane Science, 240 (2004) 187-195.

[14] L. D. Harris, B. Kim, D. J. Mooney, Open pore biodegradable matrices formed with gas foaming, J. Biomed. Mater. Res., 42 (1998) 396-402.

[15] W. L. Murphy, R. G. Dennis, J. L. Kileny, D. J. Mooney, Salt Fusion: An Approach to Improve Pore Interconnectivity within Tissue Engineering Scaffolds; Tissue Engineering, 8 (2002) 43-52.

[16] M. H. Sheridan, L. D. Shea, M. C. Peters, D. J. Mooney, Bioabsorbable polymer scaffolds for tissue engineering capable of sustained growth factor delivery, Journal of Controlled Release, 64 (2000) 91-102.

[17] L. Singh, V. Kumar, B. D. Ratner, Generation of porous microcellular 85/15 poly ($_{DL}$-lactide-co-glycolide) foams for biomedical applications, Biomaterials, 25 (2004) 2611-2617.

[18] L.M. Mathieu, T. L. Mueller, P. Bourban, D. P. Pioletti, R. Müller, J. E. Månson, Architecture and properties of anisotropic polymer composite scaffolds for bone tissue engineering, Biomaterials, 27 (2006) 905-916.

[19] L. M. Mathieu, M. Montjovent, P. Bourban, D. P. Pioletti, J. E. Månson, Bioresorbable composites prepared by supercritical fluid foaming, J. Biomed. Mater. Res., 75 (2005) 89-97.

[20] K. Partridge, X. Yang, N. M. P. Clarke, Y. Okubo, K. Bessho, W. Sebald, S. M. Howdle, K. Shakesheff, R. O. C. Oreffo, Adenoviral BMP-2 Gene Transfer in Mesenchymal Stem Cells:

In Vitro and *in Vivo* Bone Formation on Biodegradable Polymer Scaffolds, Biochemical and Biophysical Research Communications, 292 (2002) 144-152.

[21] D. Howard, K. Partridge, X. Yang, N. M. P. Clarke, Y. Okubo, K. Bessho, S. M. Howdle, K. M. Shakesheff, R. O. C. Oreffo, Immunoselection and adenoviral genetic modulation of human osteoprogenitors: *in vivo* bone formation on PLA scaffold, Biochemical and Biophysical Research Communications, 299 (2002) 208-215.

[22] X. Yang, R. S. Tare, K. A. Partridge, H. I. Roach, N. M. P. Clarke, S. M. Howdle, K. M. Shakesheff, R. O. C. Oreffo, Induction of Human Osteoprogenitor Chemotaxis, Proliferation, Differentiation, and Bone Formation by Osteoblast Stimulating Factor-1/ Pleiotrophin: Osteoconductive Biomimetic Scaffolds for Tissue Engineering, Journal of Bone and Mineral Research, 18 (2003) 47-57.

[23] J. J. A. Barry, H. S. Gidda, C. A. Scotchford, S. M. Howdle, Porous methacrylate scaffolds: supercritical fluid fabrication and *in vitro* chondrocyte responses, Biomaterials, 25 (2004) 3559-3568.

[24] J. J. A. Barry, M. M. C. G. Silva, S. H. Cartmell, R. E. Guldberg, C. A. Scotchford, S. M. Howdle, Porous methacrylate tissue engineering scaffolds: using carbon dioxide to control porosity and interconnectivity, J. Mater. Sci., 41 (2006) 4197-4204.

[25] J. J. A. Barry, S. N. Nazhat, F. R. A. J. Rose, A. H. Hainsworth, C. A. Scotchford, S. M. Howdle, Supercritical carbon dioxide foaming of elastomer/heterocyclic methacrylate blends as scaffolds for tissue engineering, J. Mater. Chem., 15 (2005) 4881-4888.

[26] X. Wang, W. Li, V. Kumar, A method for solvent-free fabrication of porous polymer using solid-state foaming and ultrasound for tissue engineering applications, Biomaterials, 27 (2006) 1924-1929.

[27] R. Butler, C. M. Davies, A. I. Cooper, Emulsion Templating Using High Internal Phase Supercritical Fluid Emulsions, Adv. Mater., 13 (2001) 1459-1463.

[28] B. D. Boyan, T. W. Hummert, D. D. Dean, Z. Schwartz, Role of material surfaces in regulating bone and cartilage cell response, Biomaterials, 17 (1996) 137-146.

[29] S. Partap, I. Rehman, J. R. Jones, J. A. Darr, "Supercritical Carbon Dioxide in Water" Emulsion-Templated Synthesis of Porous Calcium Alginate Hydrogels; Adv. Mater. 18 (2006) 501-504.

[30] Y. W. Kho, D. S. Kalika, B. L. Knutson, Precipitation of Nylon 6 membranes using compressed carbon dioxide, Polymer, 42 (2001) 6119-6127.

[31] H. Matsuyama, H. Yano, T. Maki, M. Teramoto, K. Mishima, K. Matsuyama, Formation of porous flat membrane by phase separation with supercritical CO_2, J. Membrane Sci., 194 (2001) 157-163.

[32] H. Matsuyama, A. Yamamoto, H. Yano, T. Maki, M. Teramoto, K. Mishima, K. Matsuyama, Effect of organic solvents on membrane formation by phase separation with supercritical CO_2, J. Membrane Sci., 204 (2002) 81-87.

[33] E. Reverchon, S. Cardea, E. Schiavo Rappo, Membranes Formation of a hydrosoluble biopolymer (PVA) using a supercritical CO_2–Expanded Liquid, J. of Supercritical Fluids, 45 (2008) 356-364.

[34] M. Temtem, L. M. C. Silva, P. Z. Andrade, F. Santos, C. L. Silva, J. M. S. Cabral, M. M. Abecasis, A. Aguiar-Ricardo, Supercritical CO_2 Generating Chitosan Devices with Controlled Morphology. Potential Application for Drug Delivery and Mesenchymal Stem Cell Culture. (accepted for publication in The Journal of Supercritical fluids).

[35] E. Reverchon, S. Cardea, C. Rapuan, Formation of Poly-Vinyl-Alcohol Structures by Supercritical CO_2, J. Appl. Polym. Sci., 104 (2007) 3151-3160.

[36] A. F. Ismail, L. P. Yean, Review on the Development of Defect-Free and Ultrathin-Skinned Asymmetric Membranes for Gas Separation through Manipulation of Phase Inversion and Rheological Factors, J. Appl. Polym. Sci., 88 (2003) 442-451.

[37] D. W. Hutmacher, Scaffolds in tissue engineering bone and cartilage, Biomaterials, 21 (2000) 2529-2543.

[38] D. F. Stamatialis, B. J. Papenburg, M. Gironés, S. Saiful, S. N. M. Bettahalli, S. Schmitmeier, M. Wessling, Medical applications of membranes: Drug delivery, artificial organs and tissue engineering, Journal of Membrane Science, 308 (2008) 1-34.

[39] S. V. Madihally, H. W. T. Matthew, Porous chitosan scaffolds for tissue engineering, Biomaterials, 20 (1999) 1133-1142.

[40] K. Whang, C. H. Thomas, K. E. Healy, G. Nuber, A novel method to fabricate bioabsorbable scaffolds, Polymers, 36 (1995) 837-842.

[41] K. Whang, D. C. Tsai, E. K. Nam, M. Aitken, S. M. Sprague, P. K. Patel, K. E. Healy, Ectopic bone formation via rhBMP-2 delivery from porous bioresorbable polymer scaffolds, J. Biomed. Mater. Res., 42 (1998) 491-499.

[42] G. Chen, T. Ushida, T. Tateishi, Scaffold Design for Tissue Engineering, Macromol. Biosci., 2 (2002) 67-77.

[43] S. V. Madihally, H. W. T. Matthew, Porous chitosan scaffolds for tissue engineering, Biomaterials, 20 (1999) 1133-1142.

[44] Y. S. Nam, T. G. Park, Porous biodegradable polymeric scaffolds prepared by thermally induced phase separation, J. Biomed. Mater. Res., 47 (1999) 8-16.

[45] R. Zhang, P. X. Ma, Poly(α-hydroxyl acids)/hydroxyapatite porous composites for bone-tissue engineering. I. Preparation and morphology, J. Biomed. Mater. Res., 44 (1999) 446-455.

[46] M. Sokolsky-Papkov, K. Agashi, A. Olaye, K. Shakesheff, A. J. Domb, Polymer carriers for drug delivery in tissue engineering, Advanced Drug Delivery Reviews, 59 (2007) 187-206.

[47] J. L. Drury, D. J. Mooney, Hydrogels for tissue engineering: scaffold design variables and applications, Biomaterials, 24 (2003) 4337-4351.

[48] M. Li, S. Chen, H. Yan, Preparation of crosslinked chitosan/poly(vinyl alcohol) blend beads with high mechanical strength, Green Chem., 9 (2007) 894-898.

[49] A. Jayakrishnan, S. R. Jameela, Glutaraldehyde as a fixative in bioprostheses and drug delivery matrices, Biomaterials, 17 (1996) 471-484.

[50] K. D. Yao, T. Peng, M. F. A. Goosen, J. M. Min, Y. Y. He, pH-sensitivity of hydrogels based on complex forming chitosan: polyether interpenetrating polymer network, J. Appl. Polym. Sci., 48 (1993) 343-354.

[51] M. C. Gohel, M. N. Sheth, M. M. Patel, G. K. Jani, H. Patel, Design of chitosan microspheres containing diclofenac sodium, Indian J. Pharm. Sci., 56 (1994) 210-214.

[52] D. Thacharodi, K. P. Rao, Development and *in vitro* evaluation of chitosan-based transdermal drug delivery systems for the controlled delivery of propranolol hydrochloride, Biomaterials, 16 (1995) 145-148.

[53] J. M. Ruijgrok, J. R. De Wijn, M. E. Boon, Optimising glutaraldehyde crosslinking of collagen: effects of time, temperature and concentration as measured by shrinkage temperature, J. Mater. Sci. Mater. Med., 5 (1994) 80-87.

[54]E. Lavik, R. Langer, Tissue engineering: current state and perspectives, Appl. Microbiol. Biotechnol., 65 (2004) 1-8.

[55] V. R. Sinha, A. K. Singla, S. Wadhawan, R. Kaushik, R. Kumria, K. Bansal, S. Dhawan, Chitosan microspheres as a potential carrier for drugs, International Journal of Pharmaceutics, 274 (2004) 1-33.

[56] A. R. Sarasam, R. K. Krishnaswamy, S. V. Madihally, Blending Chitosan with Polycaprolactone: Effects on Physicochemical and Antibacterial Properties, Biomacromolecules, 7 (2006) 1131-1138.

[57] P. Ducheyne, Q. Qiu, Bioactive ceramics: the effect of surface reactivity onbone formation and bone cell function, Biomaterials, 20 (1999) 2287-2303.

[58] D. A. Puleo, A. Nanci, Understanding and controlling the bone-implant interface, Biomaterials, 20 (1999) 2311-2321.

[59] V. B. Rosen, L. W. Hobbs, M. Spector, The ultrastructure of an organic bovine bone and selected synthetic hydroxyapatites used as bone graft substitute materials, Biomaterials, 23 (2002) 921-928.

[60] G. Chen, T. Ushida, T. Tateishi, Scaffold design for tissue engineering, Macromol. Biosci., 2 (2002) 67-77.

[61] H. Fukuda, Polyelectrolyte complexes of chitosan carboxymethylcellulose, Bull. Chem. Soc. Jpn., 53 (1980) 837-840.

[62] A. K. Azad, N. Sermsintham, S. Chandrkrachang, W. F. Stevens, Chitosan Membrane as a Wound-Healing Dressing: Characterization and Clinical Application, Journal of biomedical materials research, 69 (2004) 216-222.

[63] E. Mangala, T. S. Kumar, S. Baskar, K. P. Rao, Development of chitosan/Poly (vinylalcohol) blend membranes as burn dressings, Trends Biomater. Artif. Organs., 17 (2003) 34-40.

[64] O. Felt, P. Furrer, J. M. Mayer, B. Plazonnet, P. Buri, R. Gurny, Topical use of chitosan in ophthalmology: tolerance assessment and evaluation of precorneal retention, Int. J. Pharm., 180 (1999) 185-193.

[65] M. M. Amiji, Permeability and blood compatibility properties of chitosan–poly(ethylene oxide) blend membranes for haemodialysis, Biomaterials, 16 (1995) 593-599.

[66] C. H. Lee, A. Singla, Y. Lee, Biomedical applications of collagen, Int. J. Pharm., 221 (2001) 1-22.

[67] B. L. Seal, T. C. Otero, A. Panitch, Polymeric biomaterials for tissue and organ regeneration, Mater. Sci. Eng. Rep., 34 (2001) 147-230.

[68] R. D. Sayers, S. Raptis, M. Berce, J. H. Miller, Long-term results of femorotibial bypass with vein or polytetrafluoroethylene, Br. J. Surg., 85 (1998) 934-938.

[69] G. Garellick, H. Malchau, P. Herberts, The Charnley versus the Spectron hip prosthesis—clinical evaluation of a randomized, prospective study of 2 different hip implants, J. Arthroplasty, 14 (1999) 407-413.

[70] E. Fournier, C. Passirani, C. N. Montero-Menei, J. P. Benoit, Biocompatibility of implantable synthetic polymeric drug carriers: focus on brain biocompatibility, Biomaterials, 24 (2003) 3311-3331.

[71] M. Vert, G. Schwach, R. Engel, J. Coudane, Something new in the field of PLA/GA bioresorbable polymers?, J. Controlled Release, 53 (1998) 85-92.

[72] W. Chuang, T. Young, C. Yao, W. Chiu, Properties of the poly(vinyl alcohol)/chitosan blend and its effect on the culture of fibroblast *in vitro*, Biomaterials, 20 (1999) 1479-1487.

[73] S. B. Bahrami, S. S. Kordestani, H. Mirzadeh, P. Mansoori, Poly (vinyl alcohol) - Chitosan Blends: Preparation, Mechanical and Physical Properties, Iranian Polymer Journal, 12 (2003) 139-146.

[74] T. Koyano, N. Koshizari, H. Umehara, M. Nagura, N. Minoura, Surface states of PVA/chitosan blended hydrogels, Polymer, 41 (2000) 4461-4465.

[75] T. Uragami, F. Yoshida, M. Sugihara, Studies of synthesis and permeabilities of special polymer membranes. LI. Active transport of halogen ions through chitosan membranes, J. Appl. Polym. Sci., 28 (2003) 1361-1370.

[76] J. H. Kim, J. Y. Kim, Y. M. Lee, K. Y. Kim, Properties and swelling characteristics of crosslinked poly(vinyl alcohol)/chitosan blend membrane, J. Appl. Polym. Sci., 45 (1992) 1711-1717.

[77] C. Chen, F. Wang, C. Mao, C. Yang, Studies of Chitosan. I. Preparation and Characterization of Chitosan/Poly (vinyl alcohol) Blend Films, Journal of Applied Polymer Science, 105 (2007) 1086-1092.

[78] S. Gunasekaran, T. Wang, C. Chai, Swelling of pH-Sensitive Chitosan–Poly(vinyl alcohol) Hydrogels, Journal of Applied Polymer Science, 102 (2006) 4665-4671.

[79] T. Koyano, N. Koshizaki, H. Umehara, M. Nagura, N. Minoura, Surface states of PVA/chitosan blended hydrogels, Polymer, 41 (2000) 4461-4465.

[80] S. Yang, K. Leong, Z. Du, C. Chua, The design of scaffolds for use in tissue engineering. Part 1. Traditional factors, Tissue Eng., 7 (2001) 679-689.

[81] K. T. Nguyen, J. L. West, Photopolymerizable hydrogels for tissue engineering applications, Biomaterials, 23 (2002) 4307-4314.

[82] I. Adekogbe, A. Ghanem, Fabrication and characterization of DTBP-crosslinked chitosan scaffolds for skin tissue engineering, Biomaterials, 26 (2005) 7241-7250.

[83] M. J. Shamblott, J. Axelman, S. Wang, E. M. Bugg, J. W. Littlefield, P. J. Donovan, P. D. Blumenthal, G. R. Huggins, J. D. Gearhart, Derivation of pluripotent stem cells from cultured human primordial germ cells, Proc. Natl. Acad. Sci., 95 (1998) 13726-13731.

[84] S. J. Morrison, P. M. White, C. Zock, D. J. Anderson, Prospective identification, isolation by flow cytometry, and *in vivo* self-renewal of multipotent mammalian neural crest stem cells, Cell, 96 (1999) 737-749.

[85] D. Solter, J. Gearhart, Putting stem cells to work, Science, 283 (1999) 1468-1470.

[86] F. H. Gage, Mammalian neural stem cells, Science, 287 (2000) 1433-1438.

[87] K. R. Boheler, J. Czyz, D. Tweedie, H. Yang, S. V. Anisimov, A. M. Wobus, Differentiation of pluripotent embryonic stem cells into cardiomyocytes, Circ. Res., 91 (2002) 189-201.

[88] K. A. Jackson, S. M. Majka, G. G. Wulf, M. A. Goodell, Stem cells: a mini-review, J. Cell. Biochem., 38 (2002) 1-6.

[89] S. Levenberg, J. S. Golub, M. Amit, J. Itskovitz-Eldor, R. Langer, Endothelial cells derived from human embryonic stem cells, Proc. Natl. Acad. Sci., 99 (2002) 4391-4396.

II. Porous structures – Membranes and 3D-scaffolds

1. Introduction

The development of supports for tissue repair and regeneration is the base of tissue engineering.[1] These supports must present appropriate characteristics like a high porosity and good pore interconnectivity to promote cell adhesion and growth and be mechanically strong.[2,3] A commonly used material in biomedical field is chitosan, a naturally derived polymer, biocompatible and biodegradable. Even so, there are some difficulties in controlling mechanical properties and degradation rates when using this material and one of the possibilities to suppress these limitations is blending chitosan with other natural or synthetic polymer.[4] In this work, chitosan was blended with PVA, a biodegradable synthetic polymer, highly hydrophilic,[5] innocuous and biocompatible, allowing its applications in biomedical field.[6]

There are several methods available to prepare porous structures with different morphologies, including gas foaming,[7] emulsion templating,[8] phase inversion[9,10] and emulsion freeze-drying,[11] and each one of these methods presents advantages and disadvantages. The use of SCF can minimize or eliminate some of the existing problems when preparing the matrices using conventional methods, like the use of organic solvents and the necessity of post-treatment processes.[12] The most used SCF is supercritical carbon dioxide ($scCO_2$) because it is an environmentally benign solvent, non-toxic, non-flammable and with an easily accessible critical point (Tc=31.1°C and Pc=7.38 MPa). Membranes in this work will therefore be prepared using CO_2-assisted phase inversion method, where $scCO_2$ is used as non-solvent. This method will allow the preparation of sterile and ready to use devices, since CO_2 is a gas under ambient conditions and can be easily removed from the polymeric product without leaving residues and, consequently, without requiring additional post-treatments.[13] Moreover, it is possible to recover the solvent from CO_2 during depressurization and there is a

better control of membranes morphology, due to the existence of several process parameters (pressure, CO_2 flow, depressurization rate).[9,10]

Freeze-drying method was used to prepare 3D-scaffolds, to promote a high porosity and the formation of large pores.[3] All the other available methods presented some limitations and were more complexes. In this case SCFs were not used in the production of the porous structures, however to enhance biostability and mechanical properties, scaffolds were submitted to a chemical crosslinking treatment using glutaraldehyde by means of SCF technology.[14] This last step was optimized in this work, varying operation time and concentration of glutaraldehyde.

A detailed characterization of the 3D-scaffolds and membranes was made through the determination of the morphology (scanning electron microscopy), porosity (mercury porosimetry), hydrophobicity (contact angles and swelling measurements) mechanical properties (dynamic mechanical analysis) and *in vitro* biodegradability. In addition, membranes and 3D-scaffolds were evaluated in terms of cytotoxicity using International Standard guidelines[15,16] in collaboration with researchers from IST.

2. Experimental

2.1. Materials

Chitosan (75-85% deacetylated, M_w=(190-310) kg mol^{-1}), PVA (≥99% hydrolyzed, M_w=(89-98) kg mol^{-1}), absolute ethanol (purity≥99.5%), glacial acetic acid (purity≥99%), glutaraldehyde solution (50 wt.% in H_2O), phenol (purity≥95%), crystal violet, accutase™, paraformaldehyde, phosphate buffered saline (PBS) and lysozyme from chicken egg white (50,800 U/mg protein) were purchased from Sigma-Aldrich and sodium acetate tri-hydrate (purity≥99.5%) from Riedel-De-Haën. RPMI-1640 (a Roswell Park Memorial Institute medium), Dulbecco's modified essential medium low glucose (DMEM-LG), anti-Human

CD105, trypan blue and fetal bovine serum (FBS) used in cell culture were purchased from Invitrogel. L929 cells were obtained from DSMZ, Germany and WST-1 Proliferation Kit from Roche. Carbon dioxide was obtained from Air Liquid with 99.998% purity. All materials and solvents were used as received without any further purification.

2.2. Membranes preparation

The high pressure apparatus and experimental procedure used in membranes preparation was described by Temtem et al.[9,10] A schematic diagram of the high pressure apparatus is represented in Figure 2.1 and supported by a photograph of the equipment in Figure 2.2.

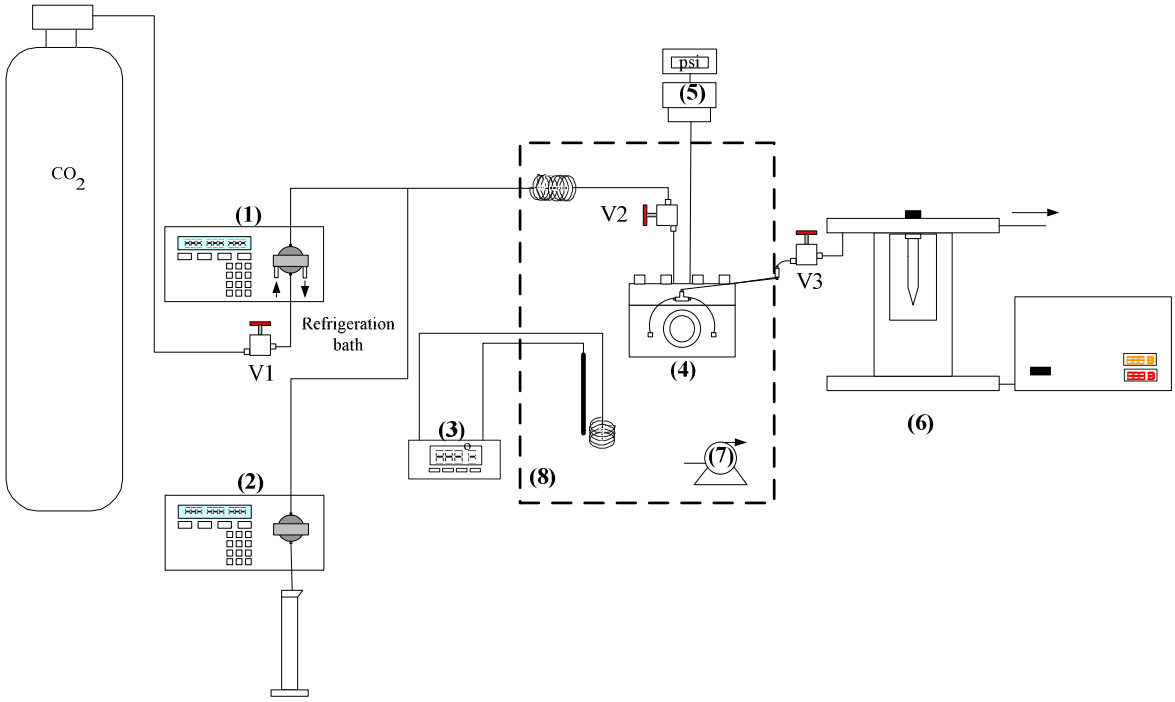

Figure 2.1 – Schematic diagram of the high pressure apparatus used where (1) Gilson 305 Piston Pump; (2) Gilson 306 Piston Pump; (3) Temperature controller (Hart Scientific, Model 2200); (4) High pressure cell; (5) Pressure transducer (Setra Systems Inc., Model 204); (6) Back pressure regulator (Jasco 880-81); (7) Water recirculating pump; (8) Visual thermostated water bath

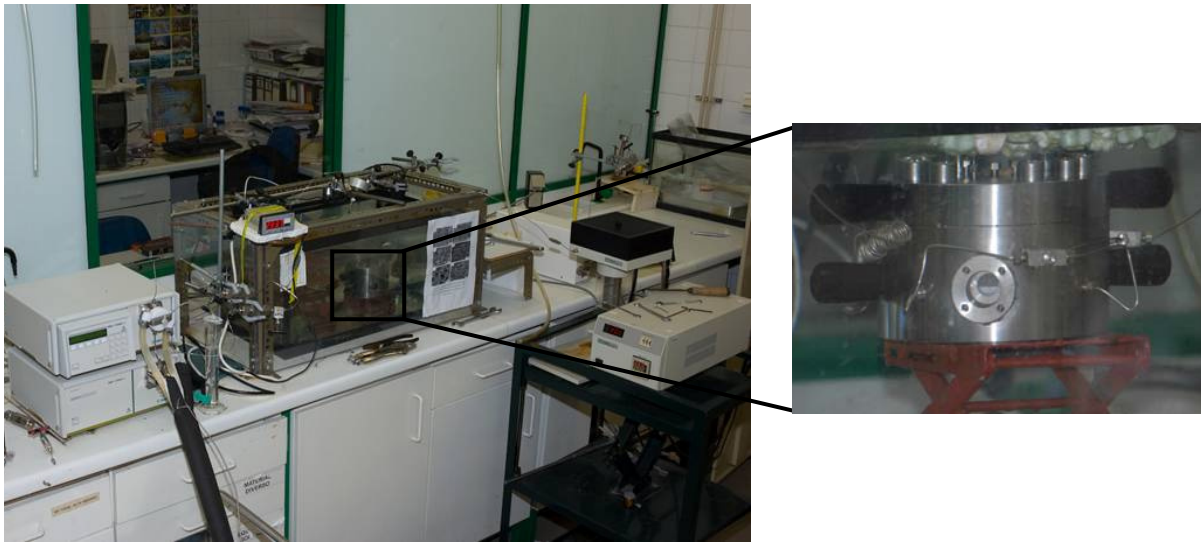

Figure 2.2 – Photograph of the experimental high pressure apparatus and detail of the high pressure cell.

The casting solution (4% w/w) is prepared dissolving chitosan and PVA in acetic acid (1% v/v) at 90ºC with stirring. The homogeneous solution at room temperature is loaded into a stainless steel cap (diameter of 68 mm and 3 mm height) and placed inside a high pressure vessel. The vessel is rapidly closed and immersed in a visual thermostated water bath at 60ºC, maintaining the temperature within ±0.01 ºC by using a controller (Hart Scientific, Model 2200). A non-solvent flow is added using two Gilson piston pumps (models 305 and 306) until 20 MPa is reached and the operation is performed in continuous mode with a constant flow rate of 4.9 g/min. The non-solvent is a binary mixture of 97.5% CO_2 and 2.5% ethanol (co-solvent) with a constant composition (isocratic mode)[17]. A back pressure regulator (Jasco 880-81) allows the control of pressure inside the vessel and the separation of CO_2 from the acetic acid used in the casting solution. The pressure inside the system is monitored with a pressure transducer (Setra Systems Inc., Model 204) with a precision of ±100 Pa.

Four membranes with different ratios of chitosan and PVA were prepared using different operation times (Table 2.1) until all the solvent is removed. After that time period, a pure CO_2 flow is passed through the system during one hour to remove the ethanol. At the end, the

system is slowly depressurized during 10 minutes and a homogeneous membrane is obtained (Figure 2.3).

Table 2.1 – Composition of membranes and operation time

Membranes	Chitosan (%)	PVA (%)	Operation time (hour)
100CHT	100	0	6
90CHT	90	10	10
75CHT	75	25	12
50CHT	50	50	16

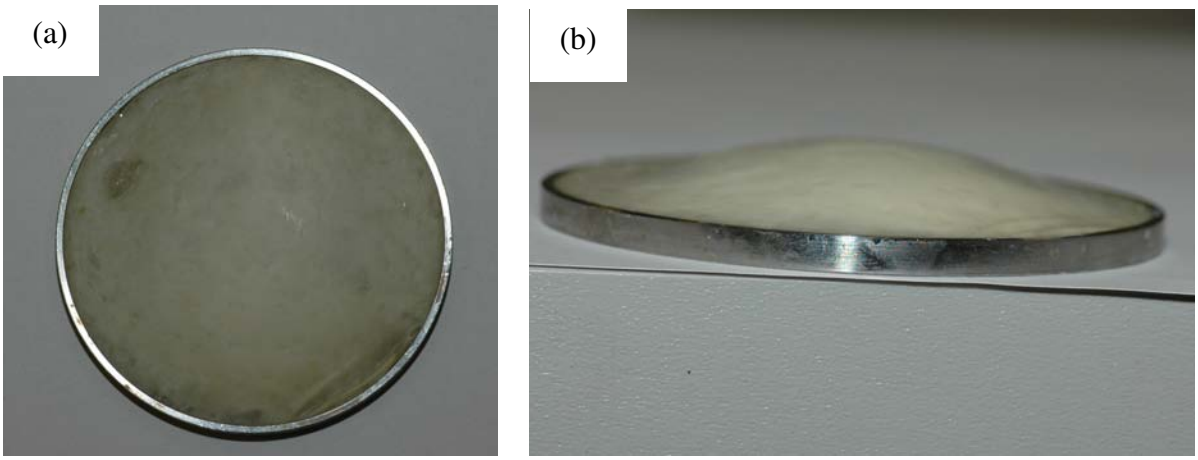

Figure 2.3 – Pictures of the chitosan membrane in the stainless steel cap immediately after preparation and removal from the high pressure cell: (a) top view and (b) lateral view.

Another simple method used for membranes production is solvent evaporation. This method was applied to prepare a membrane and to compare its properties with the properties of the membranes prepared using $scCO_2$ technology. For this membrane, it was used the same casting solution (4% w/w) and the same stainless steel cap as for the others membranes. The cap loaded with the casting solution was placed in a dryer at 60 ºC during 8 hours to

evaporate the solvent and form the membrane. In this case the prepared membrane is only composed by chitosan and defined as 100EVAP.

2.3. Scaffolds preparation

Scaffolds were prepared by freeze-drying method, as described by Madihally et al.[1] The casting solutions with concentrations of 1, 2 or 3% (w/w) are prepared dissolving chitosan and PVA in acetic acid (1% v/v) at 90ºC with stirring. The homogeneous solutions at room temperature are placed in sample tubes with an inner diameter of 1.2 cm and 3 cm height. Different sample tubes are immersed in different freezing baths maintained at -20ºC, -50ºC or -196ºC during 1 hour and lyophilized until dry in a *Telstar cryodos-50*. Refrigeration baths containing ethanol were used to obtain the temperatures of -20ºC and -50ºC and liquid nitrogen to obtain -196ºC. Table 2.2 summarizes the chitosan scaffolds (100CHT) produced for different compositions and freezing temperatures. Blended scaffolds of chitosan and PVA were prepared in the same ratios as membranes (90CHT, 75CHT and 50CHT) for the same compositions and freezing temperatures as 100CHT scaffolds.

Table 2.2 – Summary table of 100CHT scaffolds for different operation conditions

Freezing Temperature (ºC) / Composition (% w/w)	**-20**	**-50**	**-196**
1	100CHT_1% -20ºC	100CHT_1% -50ºC	100CHT_1% -196ºC
2	100CHT_2% -20ºC	100CHT_2% -50ºC	100CHT_2% -196ºC
3	100CHT_3% -20ºC	100CHT_3% -50ºC	100CHT_3% -196ºC

The scaffolds were then treated with glutaraldehyde on a high pressure apparatus similar to the one used in membranes preparation, but in this case using an additional high pressure cell where the crosslinker is placed, as represented in Figure 2.4.

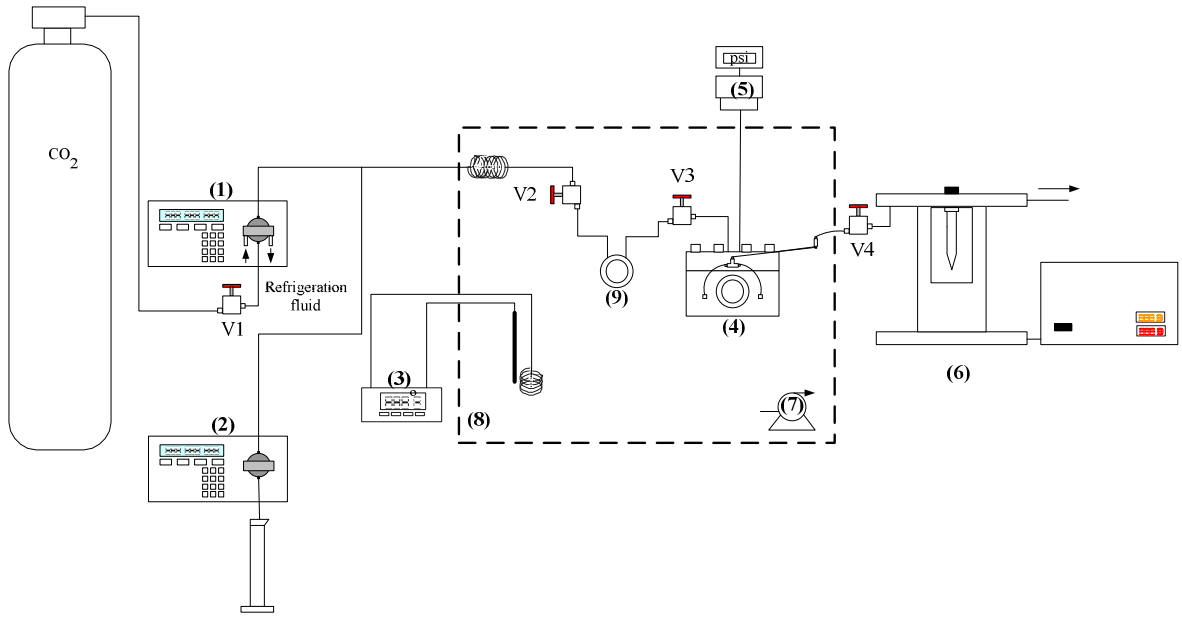

Figure 2.4 – Schematic diagram of the high pressure apparatus used where (1) Gilson 305 Piston Pump; (2) Gilson 306 Piston Pump; (3) Temperature controller (Hart Scientific, Model 2200); (4) High pressure cell containing the scaffold samples; (5) Pressure transducer (Setra Systems Inc., Model 204); (6) Back pressure regulator (Jasco 880-81); (7) Water recirculating pump; (8) Visual thermostated water bath; (9) High pressure cell containing glutaraldehyde solution

Initially, a CO_2 flow passes through the high pressure cell (9), where the crosslinker agent was placed, to saturate the CO_2 stream in glutaraldehyde. Opening the valve V3, the high pressure cell (9) is placed in contact with the high pressure cell (4), where the scaffold samples were previously sited. During a determined period of time, the CO_2 saturated in glutaraldehyde at a constant flow rate of 9.8 g/min passes through the high pressure cell (4) and contacts with the scaffold samples. Pressure (20 MPa) and temperature (40 ºC) are controlled as described in membranes preparation. After crosslinking treatment, the high

pressure cell (9) is disconnected of the system and a pure CO_2 flow passes through the high pressure cell (4) during one hour to clean the remaining residues of glutaraldehyde. At the end of operation, the system is slowly depressurized during 10 minutes.

This crosslinking process required an optimization and therefore different operation times and glutaraldehyde concentrations were tested (Table 2.3). Later on, it became necessary to increase the scaffolds diameter for cell culture tests, so a sample tube with different dimensions, an inner diameter of 1.8 cm and 4 cm height, was used and once more the operation time of the crosslinking process had to be studied (Table 2.4).

Table 2.3 – Operation conditions for crosslinking process using a sample tube with an inner diameter of 1.2 cm and 3 cm height

3D-scaffolds	Glutaraldehyde concentration (% (v/v))	Operation Time (minutes)
0.1%GTA_10min	0.1	10
1%GTA_10min	1	10
50%GTA_10min	50	10
50%GTA_1H	50	60

Table 2.4 – Operation conditions for crosslinking process using a sample tube with an inner diameter of 1.8 cm and 4 cm height

3D-scaffolds	Glutaraldehyde concentration (% (v/v))	Operation Time (minutes)
1%GTA_10min(2)	1	10
1%GTA_30min	1	30

2.4. Characterization

Morphological and physico-chemical properties

Membranes and scaffolds were characterized using scanning electron microscopy (SEM) in a Hitachi S-2400, with an accelerating voltage set to 15 kV. For cross-section analysis the samples were frozen and fractured in liquid nitrogen. All samples were coated with gold before analysis. The porosity, characteristic length values and pore size distribution were obtained in a mercury intrusion porosimeter, AutoPore IV 9500 Micromeritics. Mercury was filled progressively, changing from a filling pressure of 345 kPa to 414 MPa. Membranes hydrophobicity was evaluated through the measurement of the contact angle of water droplets in a KSV Goniometer Model CAM 100.

Mechanical properties

The dynamic mechanical analysis (DMA) experiments were performed in a Minimat firm-ware v.3.1 (Figure 2.5) using the tensile mode. The membranes were cut into strips with 2x15 mm^2 and the thickness was measured using a vernier caliper. The length between the clamps was set at 5 mm, using a full scale load of 20 N, a maximum extension of 90 mm and a speed testing of 0.1 mm/min. Measurements were performed with dry and wet membranes at room temperature. For testing in wet state, the samples were soaked in PBS solution for 1 hour and then placed in the device, being continuously wetted with this solution. Load extension graphs were obtained during testing and converted to stress strain curves applying the following equations:

$$Stress = \sigma = \frac{F}{A} \qquad (1)$$

$$Strain = \varepsilon = \frac{\Delta l}{L} \qquad (2)$$

where F - applied force, A - cross sectional area, Δl - change in length, L - length between clamps.

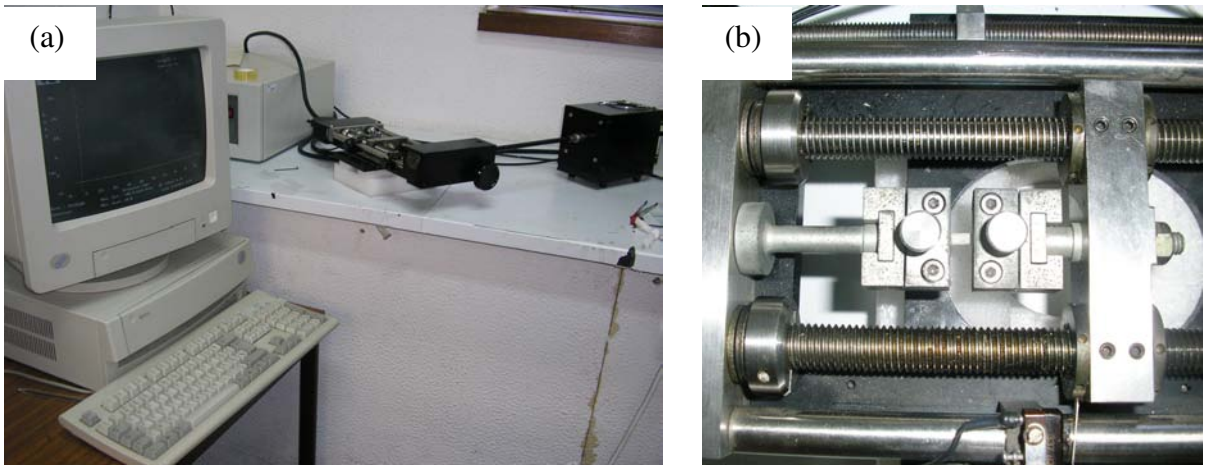

Figure 2.5 - Photograph of the (a) DMA equipment and (b) detail of the membrane sample placed between the two clamps.

Swelling measurements

The swelling tests were performed to determine the water uptake in membranes and scaffolds. Dry membrane samples were weighted and immersed in beakers containing 20 mL of PBS solution at 37ºC during 1 week. Then, the samples were weighted, after removing the excessive water. Swelling measurements for crosslinked scaffolds involved dynamic tests, using pH variations. Initially the scaffold samples were weighted and immersed in beakers containing 20 mL of PBS solution at pH 7.4 and 37ºC. Periodically, the samples were removed from the swelling medium, wiped to remove excessive water of the surface and weighted. After 24 hours, when the mass of the scaffolds reached a plateau value, the samples were transferred to a pH 5 medium (acetate buffer saline solution 0.1 M) at 37ºC. After another 24 hours, a new plateau was reached, and the samples were transferred to the pH 7.4 medium. This dynamic swelling and shrinking was studied during 5 days. Swelling degree (W (%)) of the samples was determined as defined by:

$$W(\%) = \frac{W_w - W_d}{W_d} \times 100 \qquad (3)$$

where W_d is the weight of the dried sample and W_w is the weight after immersion.

2.5. *In vitro* biodegradation studies

The degradation of membranes and scaffolds *in vitro* was studied by degrading chitosan in PBS solution at 37ºC containing 2 µg/mL of lysozyme. The concentration of lysozyme was chosen for being similar to the concentration in human serum as reported by other authors.[18,19] The initial weight of each sample was determined (W_i). After specific time intervals, samples were removed from the medium, washed with distilled water, freeze-dried and weighted. The lysozyme solution was refreshed weakly to ensure continuous enzyme activity. The extent of degradation was expressed as a percentage of remaining weight. To distinguish enzymatic degradation from dissolution, the control samples were stored under the same conditions as described above but without the addition of lysozyme. Percentage remaining weight was calculated using the following equation:

$$Remaining\ weight\ (\%) = 100 - \left(\frac{W_i - W_f}{W_i} \times 100 \right) \qquad (4)$$

where W_i is the initial dry weight of sample and W_f is the dry weight of sample after degradation.

2.6. Cytotoxicity assay

The membranes were tested for cytotoxicity following the ISO 10993-5 guidelines. Briefly, triplicates of 1 cm^2 membranes and scaffolds were placed in polystyrene tubes containing 3 mL of RPMI – 1640 with 10% (v/v) of FSB and kept in an incubator (37ºC, 5% CO_2, fully humidified) for 3 days. The liquid extracts were used to culture L929 mouse fibroblasts (initial density $80x10^3$ cells/cm^2) in 24-well plates for 2 days. The cell metabolic activity was determined by analyzing the conversion of WST-1 (light red) to its formazan derivative (dark red – absorbance at 450 nm after a 2.5 hours incubation at 37ºC) using a WST-1 Cell

proliferation kit. The results were normalized to the negative control for cytotoxicity (fresh RPMI medium) and compared to the positive control (0.01M Phenol).

In order to evaluate the effect of the direct interaction between the membranes and the L929 cells, samples were conditioned with RPMI medium (2 cm^2/mL) overnight before cell seeding in 24 well-plates (6000 cells per well). At day 3 of culture, cells cultured on the membranes were stained with crystal violet and then observed under an inverted light-phase microscope (Olympus) in order to qualitatively evaluate the morphology, cell-to-cell contact and attachment. Briefly, cells were washed with PBS solution and then stained with crystal violet (0.5% (w/v) in methanol) for 30 minutes, washed three times with PBS solution and then observed.

In scaffolds the direct interaction between the samples and the L929 cells was also evaluated. In this case, samples were conditioned with RPMI medium (2 cm^2/mL) overnight before cell seeding in 24 well-plates (6000 cells per well). At day 3 of culture, cells cultured on the scaffolds were stained with DAPI [2-(4-Amidinophenyl)-6-indolecarbamidine] and then observed by fluorescence microscopy in order to qualitatively evaluate the morphology, cell-to-cell contact and attachment. Briefly, cells were fixed with 0.5 mL of 1% paraformaldehyde for 20 minutes at room temperature and washed, once again, with PBS. Then, the cells were incubated in the dark with 0.5 mL of DAPI (1.5 µg/mL in PBS, prepared from a 1 mg/mL in PBS stock solution) for 5 minutes at room temperature, protected from light and washed again with PBS. DAPI stains blue the intact deoxyribonucleic acid (DNA) and the stained nuclei can be visualized under an ultraviolet light (Olympus U-RFLT50).

3. Results and discussion

3.1. Membranes preparation and characterization

When preparing membranes using CO_2-assisted phase inversion method several parameters have to be controlled to obtain the desired structures, namely the solvent used in the casting solution, the concentration of polymer in the casting solution, the co-solvent composition, the pressure, the temperature and the depressurization time. In this work the former process parameters were fixed to study the influence of two additional important parameters in the membranes formation: the casting solution composition and the operation time. This method has been widely studied, but was never applied to prepare blended membranes of chitosan and PVA. In this particular case the main objective is to study the influence of the PVA ratio in the morphology and in biological, mechanical and degradation properties of the prepared membranes. The variation in the operation time only happened because the casting solution composition influenced the membrane formation. So, the operation time used in each case was the enough time to obtain the membrane.

The use of SEM allows the observation of the membranes morphology and their comparison. Figure 2.6 shows the SEM images of the cross section and top view of the different membranes and it is possible to note a strong dependence of membranes morphology with the PVA ratio on the casting solution. It can be observed that 100CHT presents pores with elongated shape and with increase of PVA ratio, pores become more spherical, with smaller diameters and the membranes surface becomes irregular. Mercury porosimetry was used to complement the information about pore size and porosity of the membranes. The porosity values and characteristic length, which is an indicator of the interconnectivity between pores, for the different membranes are presented in Table 2.5. The results obtained with this technique showed that all the membranes have a low porosity, which decreases as the ratio of PVA in the casting solution increases. So, 100CHT presents a porosity of 36%,

90CHT 25%, 75CHT 22% and 50CHT 16%. The porosity values for 100CHT are similar to the ones find in literature for chitosan membranes.[20] Even so, the membranes with PVA content revealed a higher characteristic length than 100CHT. This membrane only presented a characteristic length value of 3.3 µm, while 50CHT presented 35.9 µm. These results suggests higher interconnectivity between pores in membranes with PVA content, and this fact may be related with the irregular surface and different pore shapes on these membranes as revealed in SEM images. Membranes produced by solvent evaporation, 100EVAP, and 100CHT have similar porosity values, but 100EVAP presents much less interconnectivity between pores (0.027 µm).

Table 2.5 – Influence of composition in membranes morphology

Membranes	Porosity (%)	Characteristic length (µm)
100CHT	36	3.3
90CHT	25	18.4
75CHT	22	34.4
50CHT	16	35.9
100EVAP	34	0.027

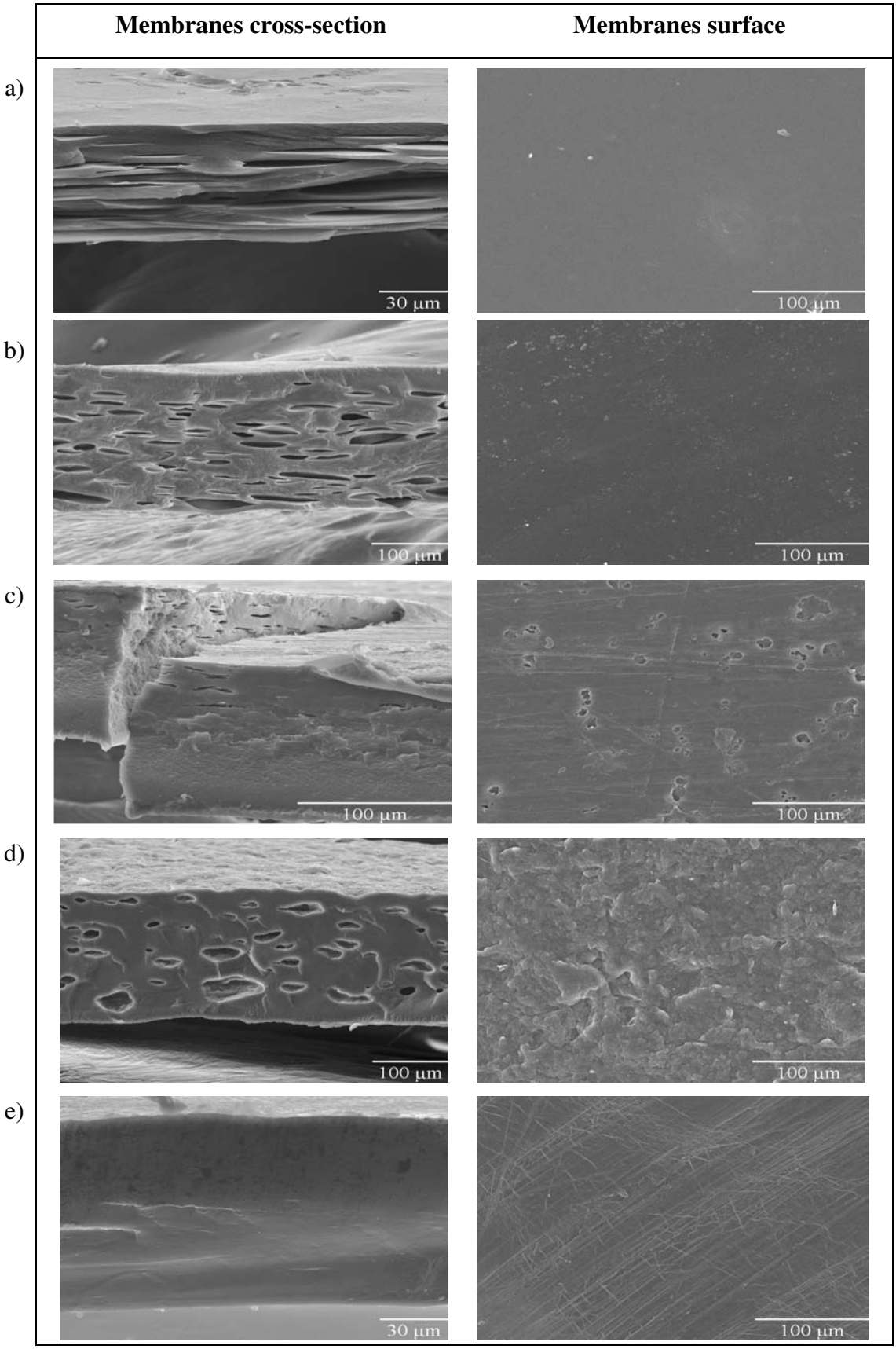

Figure 2.6 – SEM images of cross-section and surface top view of membranes with different PVA content: a) 100CHT; b) 90CHT; c) 75CHT; d) 50CHT; e) 100EVAP.

To increase the porosity of the blended membranes the process parameters could be modified. Temtem et al.[17] studied the influence of the co-solvent composition as well as the influence of the co-solvent operation mode (gradient or isocratic) in chitosan membranes morphology. An increase in the ethanol ratio in the co-solvent would increase the membranes porosity, but, for example, the use of 10% ethanol generates particles and not membranes. It was also demonstrated that the gradient mode allows the production of membranes with larger pores in comparison with the isocratic mode. Reverchon et al.[21] studied the influence of the co-solvent ratio, the process temperature and pressure on PVA membranes formation. The manipulation of these three parameters allowed the preparation of PVA membranes with different morphologies.

The CO_2-assisted phase inversion revealed to be a flexible method in membranes preparation, allowing the control of membranes morphology through the manipulation of the process parameters. In this work, chitosan and PVA blended membranes with different morphologies were prepared using this method only varying the composition of the casting solution but, as previously described, other process parameters could also be tailored to modify the membranes morphology and prepare different porous structures with interesting potential applications.

The contact angle of water droplets in the top-surface of membranes was measured to determine the relationship between membranes composition and hydrophobicity. The results presented in Table 2.6 show that there is a clear dependence between the contact angle and the PVA ratio on blended membranes. 100CHT has the most hydrophobic surface in comparison with the surface of the other prepared membranes, since it has the higher contact angle of 111º. It was also observed that the contact angle decreases with the increase of PVA content, indicating an augment of polar groups at the surface, in agreement with the fact that PVA molecules are more hydrophilic than chitosan molecules. Even so, it must be noted that

contact angle also depends on the surface roughness and porosity. In SEM images it was noticed that the membranes with PVA content have an irregular surface, particularly 50CHT, what will cause a decrease in contact angle value. Although the difference is not very significant, the membranes production method also affects the hydrophobicity of the membranes surface; when using the evaporation method (100EVAP) the contact angle of the membranes was 105º, smaller than for the membranes produced by CO_2-assisted phase inversion method (100CHT). Another publication[22] present similar values for blended films of chitosan and PVA, where the higher contact angle was obtained for chitosan films (83º) and a lower value from the blend 50% chitosan/50% PVA (56º). Chen et al. mention that although both PVA and chitosan are hydrophilic polymers, their water contact angle is still high. Considering the membranes in this work, the values are even higher and that may be associated with the hydrophobic backbone of the polymers chains, with the dense surface of membranes and/or with the polar groups at the surface.

In Table 2.6 are also included the swelling tests data obtained by determination of the water uptake in membranes. The membrane samples soaked in PBS solution (pH 7.4) at 37ºC during 1 week presented similar swelling values around (230-242)%, except for 50CHT with a higher swelling degree (284+/-7)%. Therefore, only the presence of a great amount of PVA, a highly hydrophilic polymer, will significantly increase the swelling values of membranes. These results are in accordance with the contact angle measurements, reinforcing the idea that the membranes hydrophilicity is dependent of the PVA content of the blends. Similar results for chitosan and PVA blended membranes were obtained by Mangala et al.[23]. The membrane prepared by solvent evaporation (100EVAP) partially dissolved in solution and it was not possible to determine the water uptake after 1 week.

Table 2.6 – Influence of membranes composition in contact angle and swelling degree

Membranes	Contact angle (º)	Swelling degree (%)
100CHT	111 +/- 5	236 +/- 8
90CHT	92 +/- 6	230 +/- 5
75CHT	86 +/- 4	242 +/- 6
50CHT	75 +/- 3	284 +/- 7
100EVAP	105 +/- 2	-

Membranes were submitted to tensile tests performed under dry and wet conditions to determine the influence of membranes composition in mechanical properties. These tests provide an indication of the strength and elasticity of the membranes which are important factors considering their potential applications. Figure 2.7 presents the stress-strain curves for membranes under dry and wet conditions. The tests performed in dry membranes (Figure 2.7 (a)) revealed that they all have an initial elastic behaviour for 8% strain, approximately, and after this value the stress exceeds a critical value undergoing plastic deformation. The higher stress values were supported by 100CHT, reaching 80 MPa and the elongation at break was 20%, similar to the results obtained in literature for chitosan films[24] and membranes [25]. As the PVA ratio increases, membranes revealed the ability to undergo a longer elongation at break, reaching 116% for 50CHT, but supported lower break stresses. 100EVAP presented similar stress values in comparison with 100CHT, but the strain at break was only 8%, presenting no plastic deformation. The differences between the stress-strain behaviour of dry and wet membranes are very significant. Membranes under wet conditions (Figure 2.7 (b)) revealed an exclusive elastic behaviour, with lower break stresses (1-2 MPa) and higher elongation values (72-113%) than dry membranes. The only exception is 50CHT that present both elastic and plastic behaviours and the elongation at break was similar in dry and wet states. Also, 100EVAP in wet state supported very low stress values.

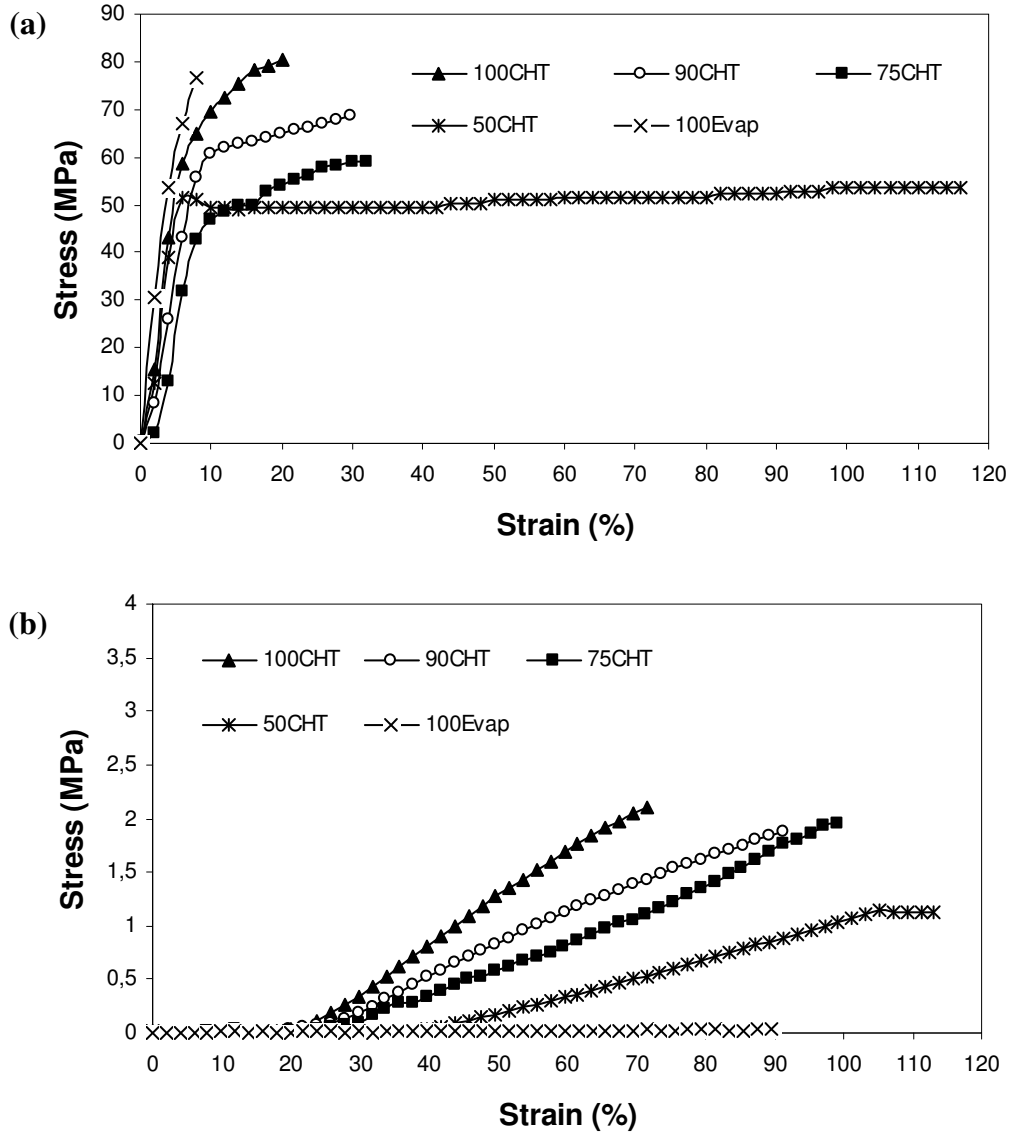

Figure 2.7 - Stress-strain curves obtained for the membranes under (a) dry conditions and (b) wet conditions (soaked in PBS during 1 hour).

The Young's modulus or elastic modulus (E) is a mechanical parameter that gives information about membranes stiffness and it is defined as the slope of the stress-strain curve (E=stress/strain) in the elastic deformation region. The results presented in table 2.7 shows that the stiffness depends of the membranes composition and, as expected, the Young's modulus values are lower in wet state than in dry state. The values obtained for 100CHT in dry and wet states are in agreement with the data from literature[24,25]. The blended membranes

presented lower values of Young's modulus as the ratio of PVA increases, except for 50CHT in dry state. A possible explanation for this fact is that the membrane 50CHT presents a very low porosity and an irregular surface, affecting the membrane response to the tensile tests.

Table 2.7 – Influence of membranes composition in Young's modulus

Membranes	Young's modulus (MPa)	
	Dry state	Wet state
100CHT	1075	4.3
90CHT	729	2.8
75CHT	709	2.6
50CHT	906	1.6
100EVAP	1338	0.03

3.2. Scaffolds preparation and characterization

3D-scaffolds were prepared using freeze-drying method in order to obtain high porous structures. In this method, as in others, the operation parameters must be controlled to produce matrices with the desired properties in accordance with their application. The freezing temperature, polymer percentage and composition of the casting solution are some of the parameters that affect the morphology and may influence the biological, mechanical and degradation properties of the scaffolds. So, different scaffolds were prepared and studied for freezing temperatures of -20ºC, -50ºC and -196ºC, with different PVA ratios and using 1, 2 and 3% (w/w) of the casting solution.

Initially, the effect of the casting solution concentration was evaluated, for a constant composition (75%CHT/25%PVA) and a freezing temperature of -196ºC. The results of mercury porosimetry for casting solutions with concentrations of 1, 2 and 3% (w/w) revealed

similar pore size diameters, as well as porosity and characteristic length values (Table 2.8). The main difference between these structures is their stiffness behaviour that increases with higher polymer content. In literature it is said that the mechanical properties of the matrices should match those of the tissue at the implantation site or at least protect the cells from compressive or tensile forces that may damage them[1]. Therefore, the 3D-scaffolds prepared with 3% (w/w) of the casting solution were used in the following studies due to its stiffness structure, appropriate for most biomedical applications.

Table 2.8 – Influence of the casting solution concentration in pores morphology of 3D-scaffolds

3D-scaffolds	Porosity (%)	Characteristic length (µm)
75CHT_1% -196ºC	93.3	34.6
75CHT_2% -196ºC	93.2	34.9
75CHT_3% -196ºC	91.8	36.4

For the same composition and concentration of the casting solution (100CHT and 3% (w/w)) and different freezing temperatures, scaffolds prepared at -20ºC have bigger pores than the scaffolds prepared at -50ºC and -196ºC (Figure 2.8 (a)). The distribution of pore size diameter for a freezing temperature of -20ºC presents a maximum at 40.6 µm, while for -50ºC and -196ºC the higher values were 11,3 µm and 13,9 µm, respectively. Facing these results, the subsequent experiences were made using freezing temperatures of -20ºC. At this temperature it is possible to obtain scaffolds with bigger pores, which will help to promote cell adhesion and growth and allow nutrient delivery, waste removal, protein transport, gaseous exchange, and general vascularisation. These aspects are described in literature as essential in scaffolds design.[26]

The objective at this moment is to determine the effect of the PVA ratio in 3D-scaffolds pore size, keeping a constant freezing temperature of -20ºC and the casting solution with polymer concentration of 3% (w/w). The results in Figure 2.8 (b) show that 100CHT present the higher values of pore size diameter followed by 90CHT with 40.62 µm and 32.91 µm, in that order. In comparison with these results, 75CHT and 50CHT present smaller pores, although larger distributions, showing a wide range of pores size. In addition, $scCO_2$-assisted crosslinking with glutaraldehyde showed no influence on pores morphology of the scaffolds.

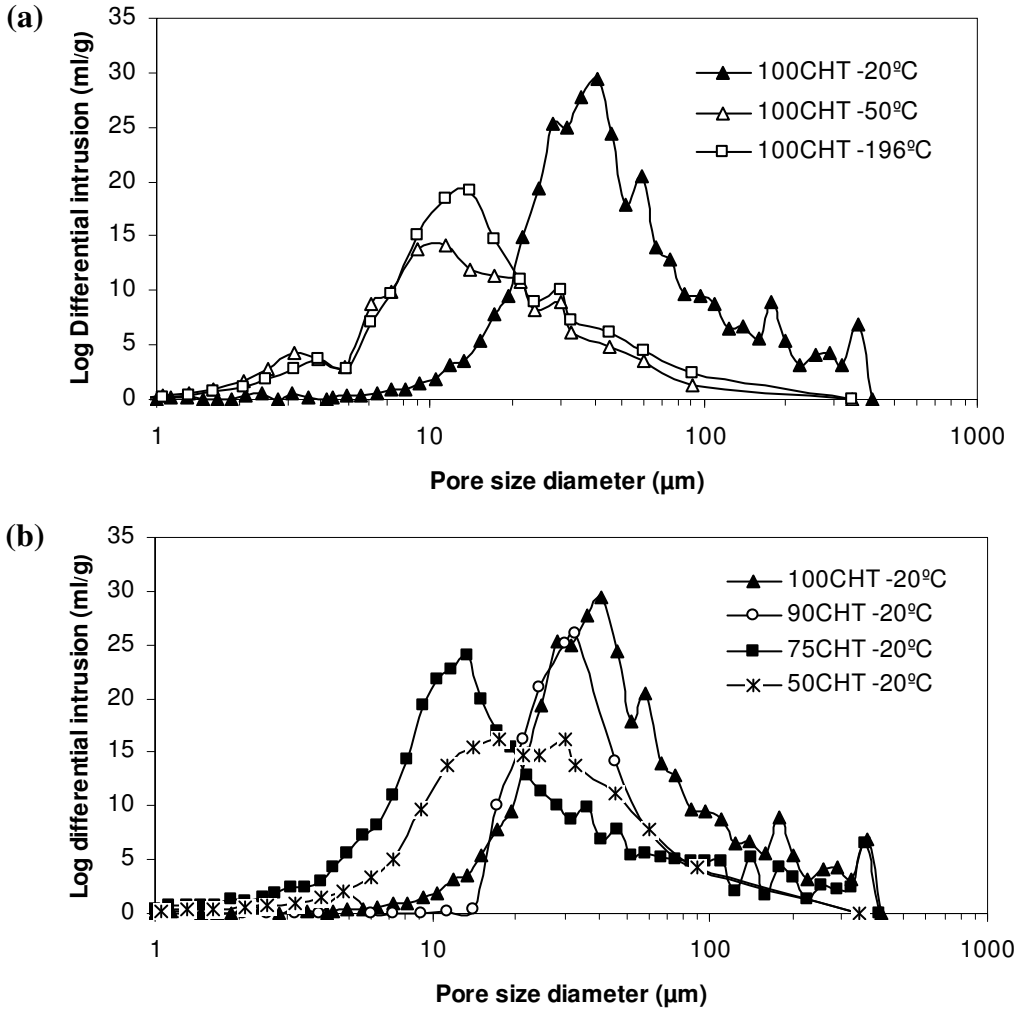

Figure 2.8 – Influence of: (a) freezing temperature and (b) composition in the pore size diameter of 3D-scaffolds prepared with 3% (w/w) of polymer.

Figure 2.9 (a) is a picture of a scaffold sample prepared at -20ºC and using the casting solution with 3% (w/w) of polymer concentration, where it is possible to observe the high porosity of the structure. The SEM images in Figure 2.9 (b) and (c) allows the observation of the pores morphology in different regions of another scaffold sample prepared at -50ºC and using the casting solution with 3% (w/w) of polymer concentration. There were observed no significant differences in the pores morphology for scaffolds prepared at different freezing temperatures. It was also noticed that the blended structures with PVA in their composition, were less rigid than the chitosan scaffolds and observing the SEM images in Figure 2.9 it is possible to note the difference between scaffolds with and without PVA.

The dynamic swelling tests were performed to determine the water uptake in crosslinked scaffolds and study their response to pH variations. The scaffolds were prepared in sample tubes with an inner diameter of 1.2 cm and 3 cm height using a casting solution with 3% (w/w) concentration and a freezing temperature of -50ºC. The prepared scaffolds were treated using CO_2-assisted crosslinking process with different glutaraldehyde concentrations and different operation times, as previously described in Table 2.2. The effect of pH variations in swelling has been studied for chitosan and PVA blended hydrogels[27] and similar results were obtained for the scaffolds in this work. In literature it is said that when chitosan hydrogels are placed in a buffer solution with a pH below its pK_a (<6.3) there will be an ionization of primary amine groups in chitosan. The $–NH_2$ groups of chitosan are positively charged ($–NH_3^+$) and this attracts and creates a higher concentration of counterions (Ac^-) inside the hydrogel and results in a new osmotic pressure inside and outside of the hydrogel. These positive charges also provide electrostatic repulsion forces, which contributes to the expansion of the hydrogel network. For a swelling medium with pH values higher than pK_a of chitosan, the originally ionized groups in the gel matrix gradually lose their charges and, therefore, lose their attraction for couterions, eliminating the osmotic pressure difference, and the gel matrix contracts[27].

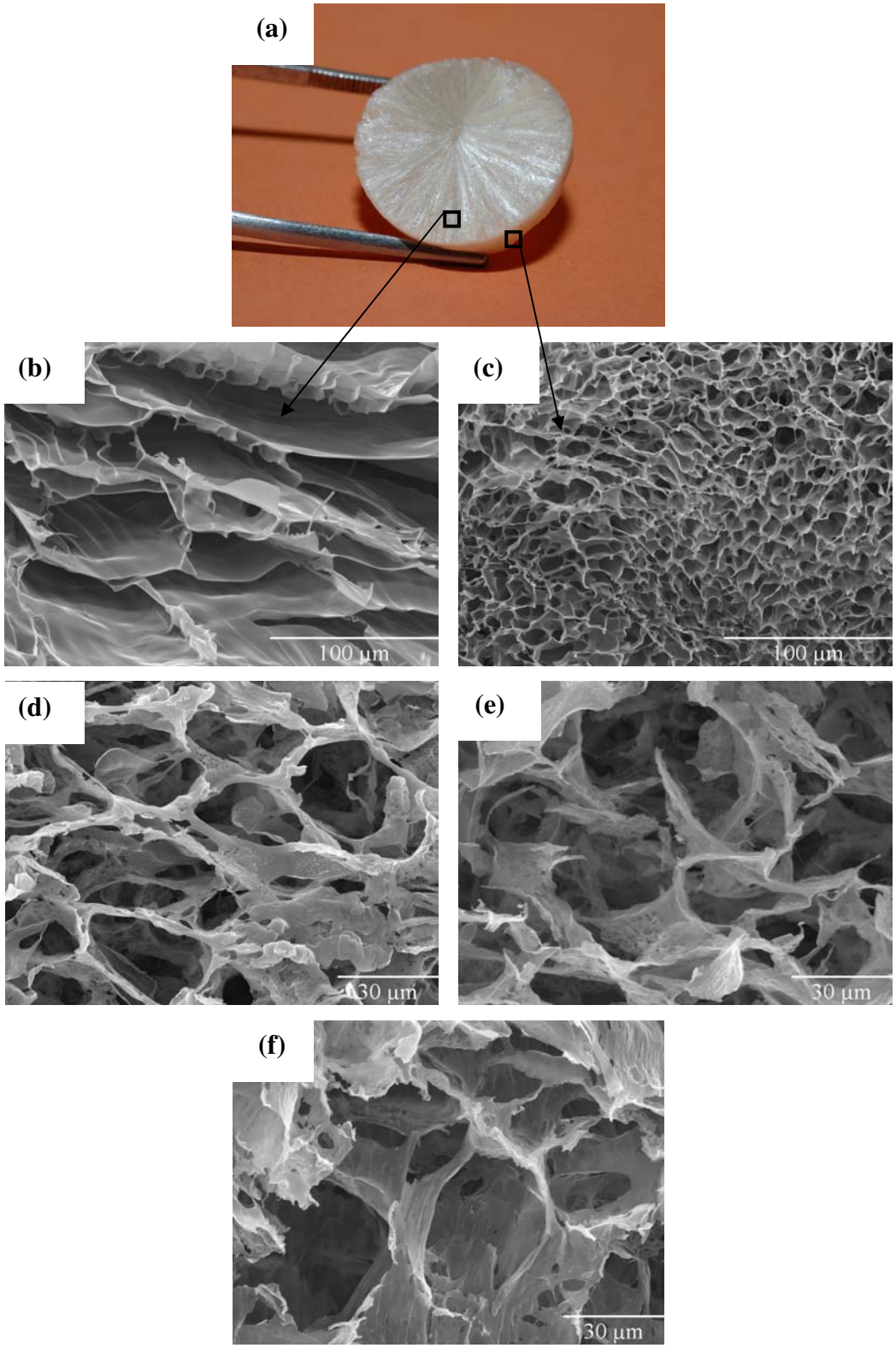

Figure 2.9 – 3D-scaffolds prepared with 3% (w/w) of polymer in the casting solution: (a) picture of chitosan scaffold frozen at -20ºC (100CHT_3% -20ºC); (b) and (c) SEM images of chitosan scaffold frozen at -50ºC (100CHT_3% -50ºC) from two different regions; and SEM images of blended scaffolds frozen at -20ºC with: (d) 90% chitosan (90CHT_3% -20ºC), (e) 75% chitosan (75CHT_3% -20ºC) and (f) 50% chitosan (50CHT_3% -20ºC).

The results of the dynamic swelling tests in chitosan scaffolds are presented in Figure 2.10. The scaffolds that were crosslinked with 50% glutaraldehyde during 1 hour and during 10 minutes (50%GTA_1H and 50%GTA_10min, respectively) presented low variations in swelling degree for different pH values. The swelling values for 50%GTA_1H were between 1700% (pH 7) and 2000% (pH 5). The 3D-scaffolds treated with 0.1% of glutaraldehyde during 10 minutes (0.1%GTA_10min) began to dissolve, losing their weight along time. So, in the first 48 hours they showed a high swelling capacity, reaching 6848% at pH 5, but after 96 hours the swelling value decreased to 4000% (pH 5), as a result of the scaffold dissolution. 1%GTA_10min scaffold exhibited the expected swelling results, as the crosslinking treatment was enough to stabilize the structure but did not disable the scaffolds response to pH variations. The swelling values were around 1400%-1600% for pH 7 and 4100%-4500% for pH 5.

The glutaraldehyde crosslinking treatment was used to enhance the biostability and the mechanical properties of the scaffolds, but a high concentration of the crosslinker will consume all the amino groups of chitosan in the crosslinking reaction, limiting the scaffolds response to pH stimulus. In the other hand, a low concentration of glutaraldehyde will be inefficient and the scaffolds will dissolve in solution, as it was verified for 0.1%GTA_10min. The crosslinking time also influenced the results and the scaffolds that were crosslinked for 1 hour revealed to be the less sensitive to pH variations. Even so, 10 minutes appear to be enough time to uniformly crosslink the scaffolds.

These swelling tests were initially performed in chitosan scaffolds that were freeze-dried at -50ºC. Morphological tests that were subsequently carried out have shown that a freezing temperature of -20ºC allows the formation of scaffolds with larger pores, as described in this work. For this reason, the next swelling tests were performed in scaffolds frozen at -20ºC.

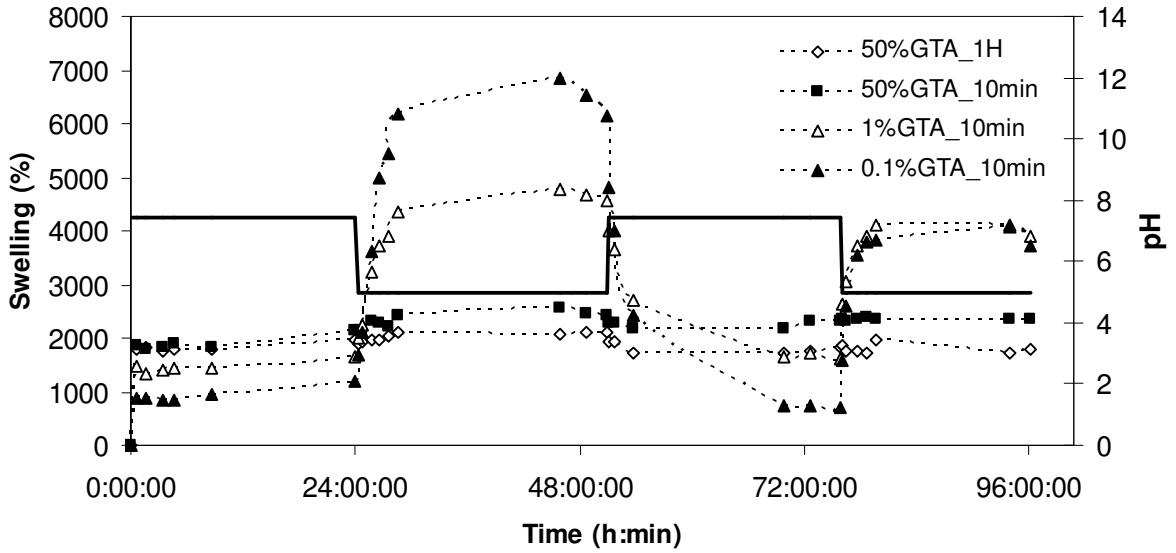

Figure 2.10 – Dynamic swelling of 3D-scaffolds with 3% (w/w) of chitosan, frozen at -50ºC, crosslinked with different glutaraldehyde concentrations and using different operation times.

The necessity to increase the scaffolds diameter for use in cell tests (sample tube with an inner diameter of 1.8 cm and 4 cm height) required an optimization in the crosslinking process. The optimal concentration of glutaraldehyde was determined in previous swelling tests as being 1% (v/v) but it was necessary to determine the appropriate operation time for these scaffolds. So, scaffolds crosslinking process was studied for 10 minutes and 30 minutes. The scaffolds crosslinked during 10 minutes (1%GTA_10min(2)) shown a great loss of mass after two days in PBS solution, while the 30 minutes crosslinked structures (1%GTA_30min) did not show significant differences. Therefore the following swelling tests were performed using the scaffolds crosslinked with 1% (v/v) of glutaraldehyde during 30 minutes.

Figure 2.11 presents the results for the water uptake measurements on blended scaffolds. The swelling values obtained for 100CHT were the highest, around 2700%-2900% at pH 5, and decreased with the increase of PVA ratio. It was observed that 100CHT kept the appearance during swelling tests, while blended scaffolds lost some weight, mainly 50CHT. These results indicate that the crosslinking process was less efficient for scaffolds with PVA

content and, by the fact that PVA is a highly water soluble polymer, causes faster weight losses of these scaffolds. Even so, only 50CHT presents significant weight losses affecting the swelling results. Gunasekaran et al.[27] studied the effect of the PVA content on the dynamic swelling of chitosan and PVA blended hydrogels. It was described that the PVA content shows no effect on the swelling values, because PVA does not have any ionisable groups in its molecular structure at any buffer pH value. This fact explains the decrease in swelling ratio as the PVA content of scaffolds increases, given that only chitosan is affected by the pH variations.

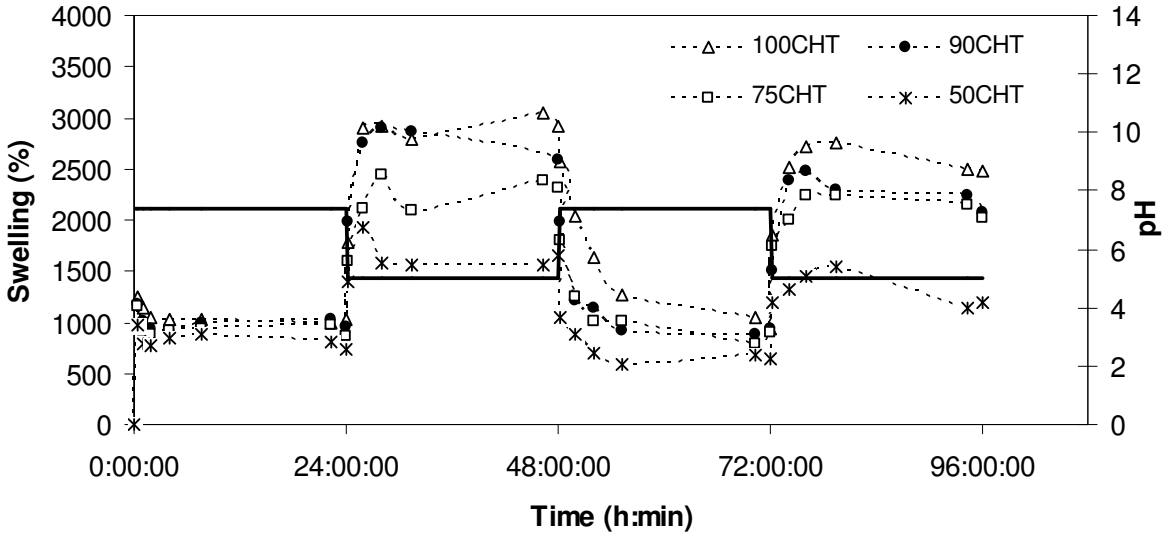

Figure 2.11 – Dynamic swelling of 3D-scaffolds prepared with 3% (w/w) of polymer (chitosan+PVA), frozen at -20ºC, crosslinked with 1% (v/v) of glutaraldehyde during 30 minutes and using different PVA ratios.

3.3. *In vitro* biodegradation studies

In vitro degradation tests were performed using lysozyme, an enzyme present in the human body and produced by macrophages during wound healing. Lysozyme degrades chitosan and permits the resorption of the scaffold, which is incorporated into the extracellular matrix for the rebuilding of physiological normal tissues[26]. Samples of each membrane and scaffold were soaked in PBS solution containing lysozyme and their remaining weight was measured

along time to determine the degradation of these structures. Additionally, other samples were soaked in PBS solution but without the addition of the enzyme, to distinguish the degradation kynetics with and without the presence of lysozyme.

Figure 2.12 (a) shows that in PBS solution the remaining weight decreased mainly in the first week and depended on the PVA content. This fact implies that some of the PVA content dissolves in solution. In PBS solution with lysozyme, degradation occurs along the time, even after the first week, mainly for 100CHT and 75CHT, where the membranes degradation can be clearly observed by the reduction of weight (Figure 2.12 (b)). Comparing the two graphs, all the membranes placed in PBS solution with lysozyme presented a lower percentage of remaining weight after 30 days of degradation in comparison with membranes in PBS solution without lysozyme. The great reduction of membranes weight in the first week occurred because the pores allow the diffusion of the lysozyme into the matrix and, after some days of degradation, the pores collapse and less area is exposed to enzyme degradation. 90CHT membranes presented a low degradation rate even after 30 days in PBS solution with lysozyme as observed in Figure 2.12 (b), but the SEM images in Figure 2.13 show that the degradation occurred and there was a collapse of the porous structure. For 100EVAP the remaining weight after 3 days in PBS solution was around 20% and in the presence of lysozyme only 2%, while the membranes prepared using CO_2-assisted phase inversion method permitted the preparation of devices that kept more than 70% of their initial weight after 30 days of degradation. Normally, post-treatment processes are used to prevent structures dissolution what may carry some disadvantages. In this case, the use of supercritical technology allows the preparation of ready to use membranes without the necessity of any further treatments.

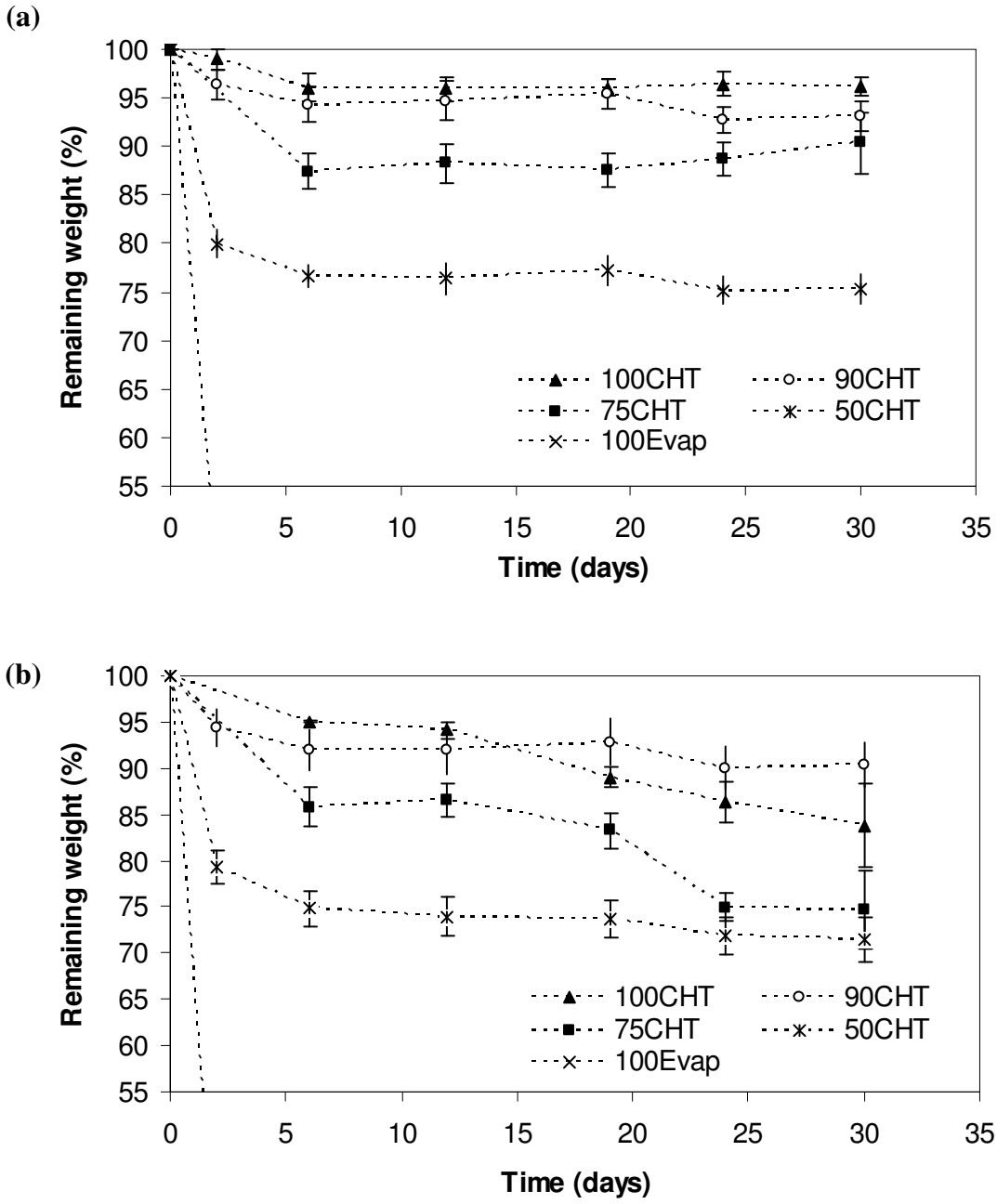

Figure 2.12 – Degradation curves of membranes in (a) PBS solution and (b) PBS solution containing lysozyme.

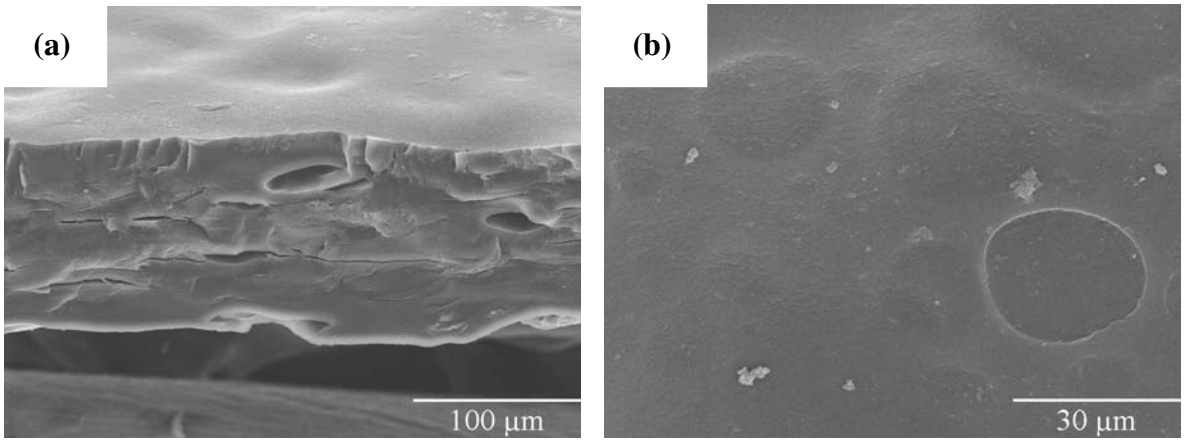

Figure 2.13 – SEM images of 90CHT membranes after 30 days in PBS solution containing lysozyme: (a) cross section (300x) and (b) surface top view (1000x).

The degradation tests performed in crosslinked scaffolds 1%GTA_30min (crosslinking procedure during 30 minutes using glutaraldehyde with 1% (v/v)) revealed similar results as for membranes: PVA content of the scaffolds affected their degradation rate. In Figure 2.14 (a) it is possible to note the same initial decrease of scaffolds weight as happened for membranes, which is probably due to the PVA dissolution in aqueous medium. In the presence of lysozyme as shown in Figure 2.14 (b) the degradation of the scaffolds occurs along the time and after 30 days the remaining weight is much lower than for the scaffolds placed in PBS solution without the enzyme. For example, after 30 days of degradation, 50CHT placed in PBS solution presented 67% of remaining weight, while in PBS solution with lysozyme the corresponding value was 31%. Scaffolds are very porous structures what allows the diffusion of lysozyme into the matrices and their higher degradation when compared with membranes and leading to a decrease of the remaining weight along time. SEM images in Figure 2.15 presents the 100CHT scaffold after 65 days in PBS solution containing lysozyme and confirms the degradation results.

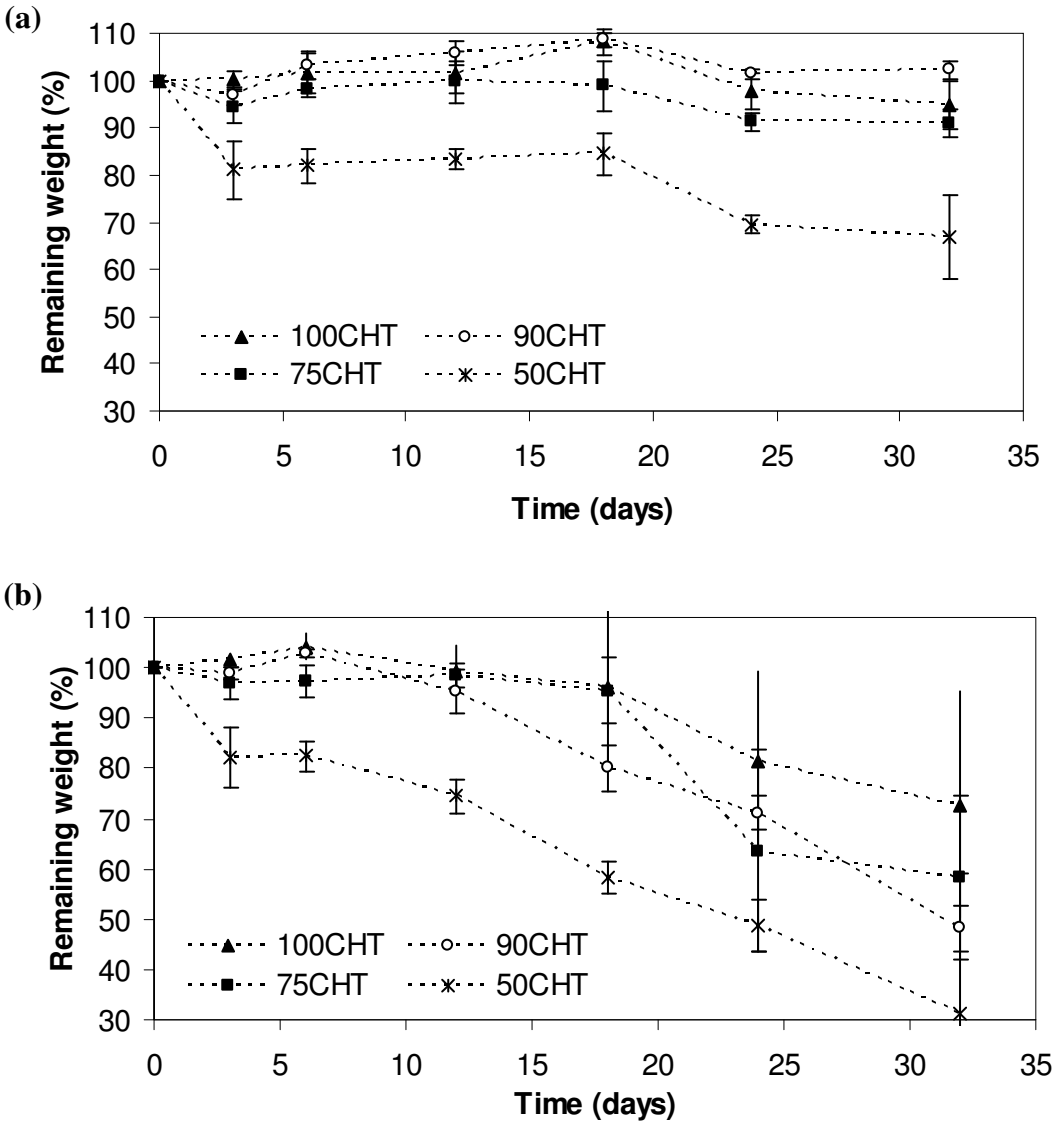

Figure 2.14 – Degradation curves of 3D-scaffolds prepared with 3% (w/w) of polymer (chitosan+PVA), frozen at -20ºC, crosslinked with 1% (v/v) of glutaraldehyde during 30min and using different PVA ratios in (a) PBS solution and (b) PBS solution containing lysozyme

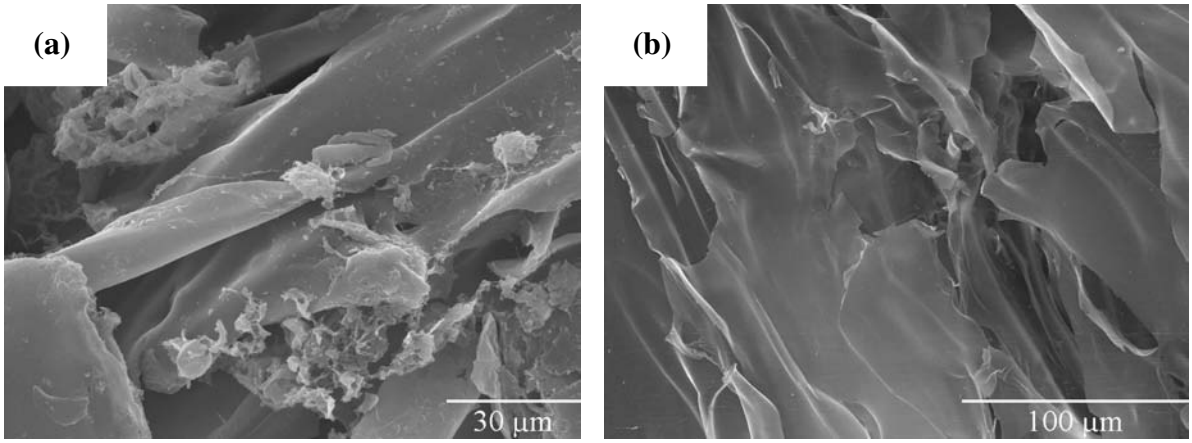

Figure 2.15 – SEM images of 3D-scaffold prepared with 3% (w/w) of chitosan, frozen at -20ºC and crosslinked with 1% (v/v) of glutaraldehyde during 30min after 65 days in PBS solution containing lysozyme in different regions and using different magnifications (a) 800x and (b) 400x.

3.4. Cytotoxicity assay

The cytotoxicity tests evaluate the cell responses when interacting with the materials, which is an essential aspect in tissue engineering and regenerative medicine. Membranes with different compositions and scaffolds with different crosslinking concentrations and operation time were tested.

Figure 2.16 presents images of L929 fibroblast cells cultured in membranes and in polystyrene (control) after 3 days in culture. It is possible to observe that cells cultured on 100CHT presented their characteristic fibroblastic morphology (spindle shaped), while the cells on 50CHT presented a spherical morphology and no cell-cell contact. Table 2.9 summarizes the response of L929 fibroblast cells cultured in the membranes, according to the images in Figure 2.16 and presenting the cell attachment, morphology, proliferation and cell-cell contact results.

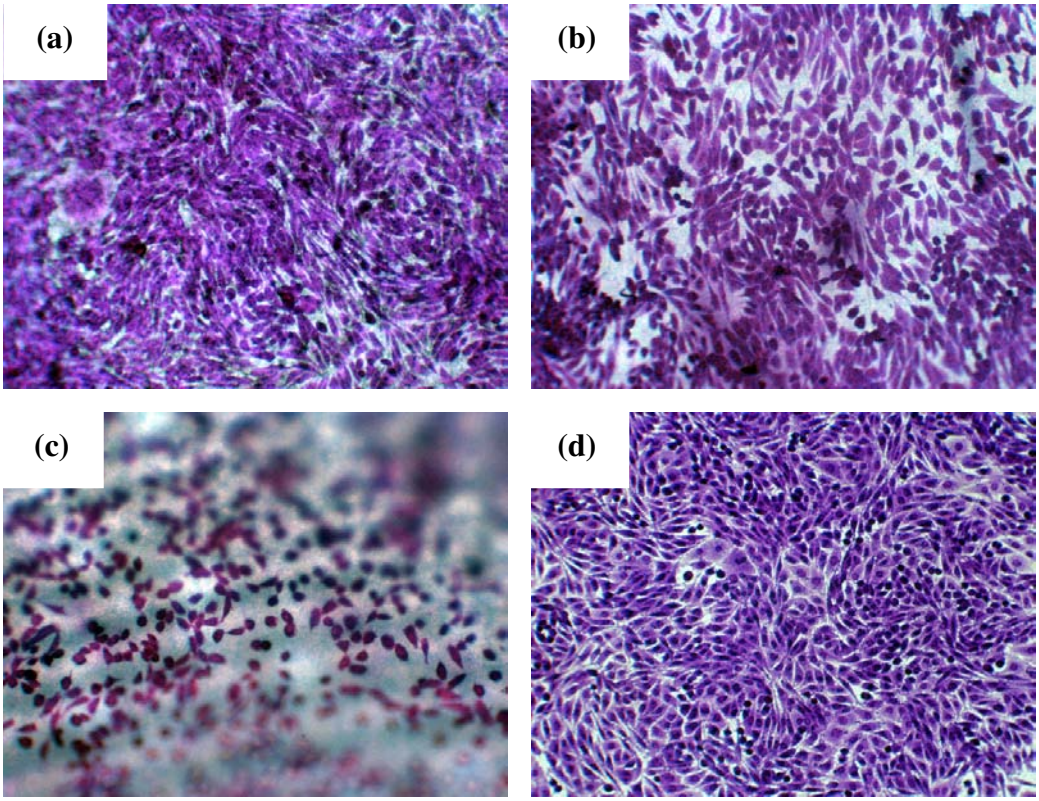

Figure 2.16 – Representative images of L929 fibroblast cells cultured in (a) 100CHT, (b) 75CHT, (c) 50CHT and (d) polystyrene control after 3 days in culture, presenting their characteristic morphology.

Table 2.9 – Response of L929 fibroblast cells cultured in the membranes

	100CHT	**75CHT**	**50CHT**
Cell Attachment	+++	+++	+/-
Cell Morphology	+++	++	+/-
Cell-Cell Contact	+++	+	-
Cell Proliferation	+++	++	+/-
Cell Penetration	N/A	N/A	N/A

Figure 2.17 presents the metabolic activity of the L929 cells (normalized to control) after 48 hours of culture with medium extracts of the different membranes. No cytotoxic effect was observed for any of the membranes prepared, when compared to commonly used tissue culture grade polystyrene (negative control). The 90CHT membranes were not tested, but none of the other membranes that contain higher concentrations of PVA in their composition presented cytotoxicity. So, we may predict that these membranes will not present cytotoxic effects. In addition, the obtained results are in agreement with previously reported data attesting the non cytotoxicity of PVA/chitosan blended materials, containing 40% of chitosan and 60% of PVA in their composition[28].

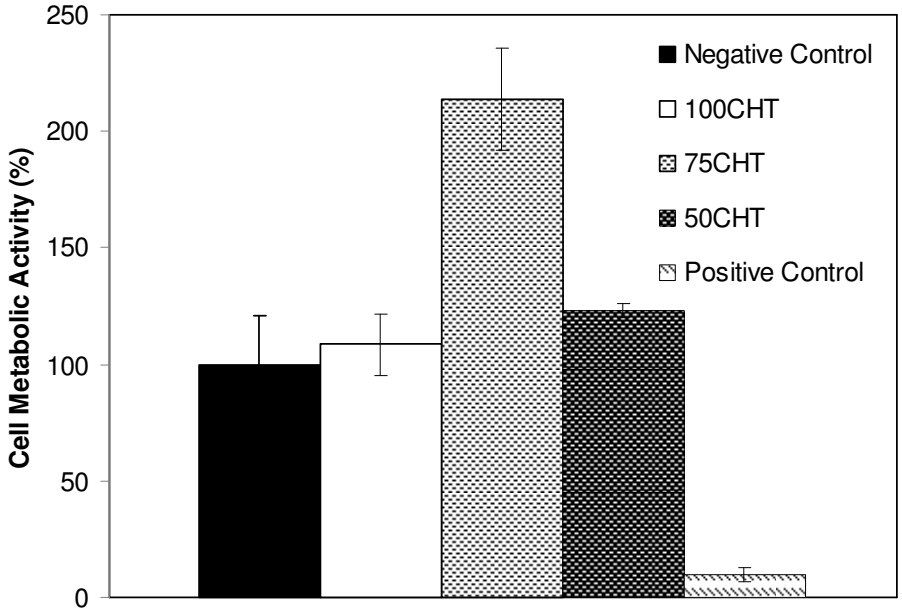

Figure 2.17 – Cytotoxicity tests of the membranes following the ISO standards for biomaterials. Negative control: tissue culture plate control (polystyrene); Positive control: 0.01 M phenol.

The chitosan scaffolds that were submitted to a $scCO_2$-assisted crosslinking treatment were tested for cytotoxicity using the direct method. The effects of the glutaraldehyde concentrations and the operation time in the toxicity were evaluated.

Figure 2.18 presents representative images of L929 fibroblast cells cultured in the scaffolds and in polystyrene (control) after 3 days in culture. To complete this information, Table 2.10

summarizes the response of L929 fibroblast cells cultured in the scaffolds, presenting the cells attachment, proliferation and penetration. The results for scaffolds with a high concentration of glutaraldehyde and 1 hour of crosslinking treatment (50%GTA_1H) revealed that the cell response was affected (in the perifery some cell death was found), while the other scaffolds presented positive results with no visible cytotoxic effect on cells. The most positive results were observed for 1%GTA_10min, with a good cell attachment, proliferation and penetration, confirmed by the images, where it is possible to observe the presence of cells in different places inside the scaffold. These results are in agreement with the data reported by Chen et al.[14] where the use of $scCO_2$ is able to remove the entire remaining glutaraldehyde using a dynamic process, because of the high solubility of glutaraldehyde in $scCO_2$.

Therefore, the non-cytotoxicity of the membranes and scaffolds enables their potential use as scaffolds to sustain human stem cell adhesion and proliferation *in vitro*.

Table 2.10 – Response of L929 fibroblast cells cultured in the 3D-scaffolds

	0.1%GTA_10min	**1%GTA_10min**	**50%GTA_10min**	**50%GTA_1H**
Cell Attachment	++	++	+	+/-
Cell Morphology	N/A	N/A	N/A	N/A
Cell-Cell Contact	N/A	N/A	N/A	N/A
Cell Proliferation	+	++	+	+/-
Cell Penetration	+	++	+	+/-

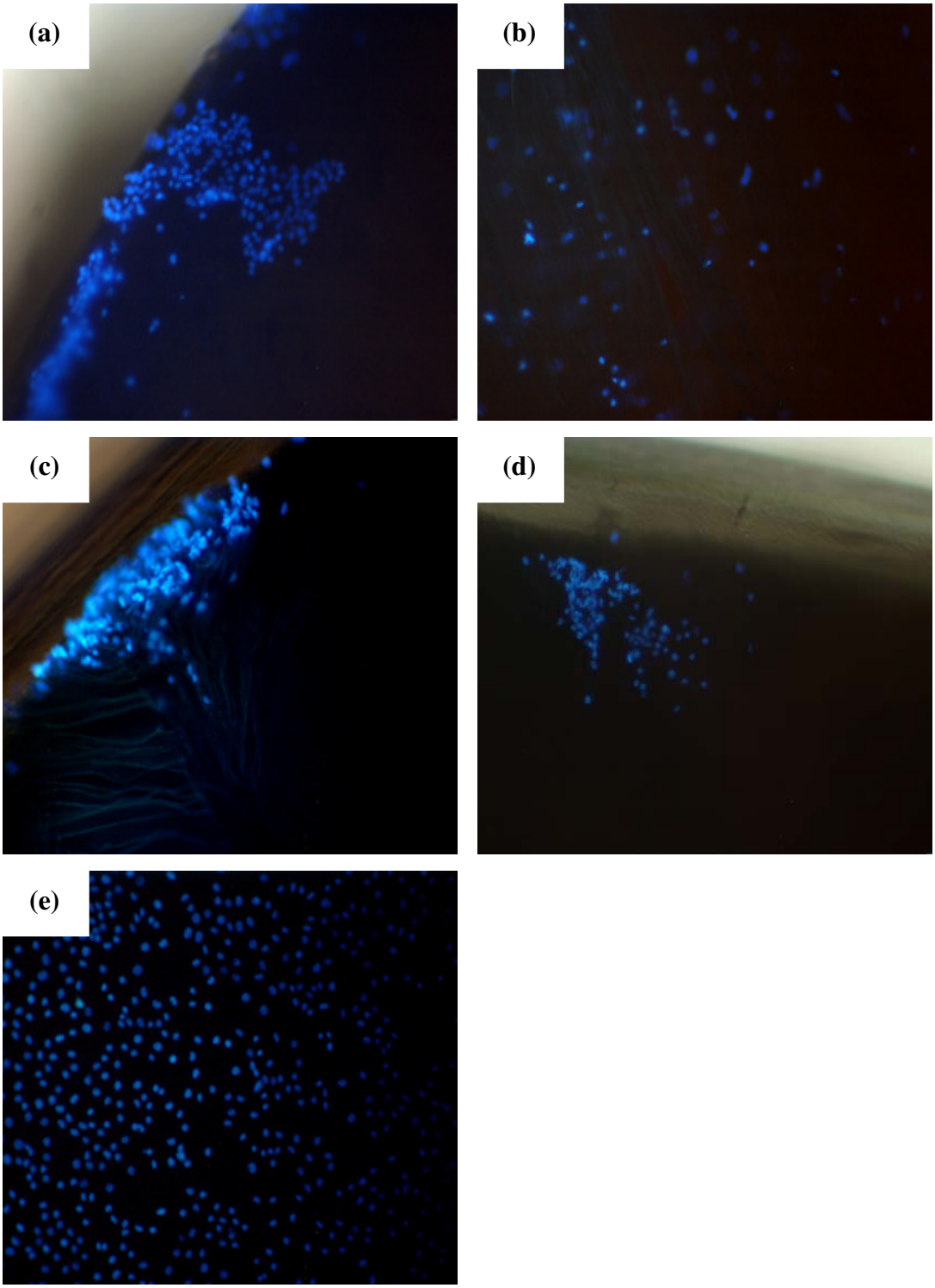

Figure 2.18 – Representative images of L929 fibroblast cells cultured in (a) 0.1%GTA_10min, (b) 1%GTA_10min, (c) 50%GTA_10min, (d) 50%GTA_1H and (e) polystyrene control after 3 days in culture.

4. Conclusions

This study has shown that it is possible to prepare stable and sterile chitosan and PVA blended membranes and 3D-scaffolds with potential use as tissue engineering scaffolds, taking advantage of the SCF technology.

The versatility of $scCO_2$-assisted phase inversion method allows the preparation of structures with different morphologies by varying the process conditions. In this work one of the main objectives was to study the influence of different chitosan/PVA ratios in membrane properties. The results showed that by adjusting the casting solution composition it was possible to modify the morphology, the hydrophilicity and the mechanical properties of the membranes. SEM and mercury porosimetry of these structures showed that the presence of PVA in the membranes composition causes a decrease in porosity values and an increase in pores interconnectivity. This dependence was also verified for the contact angle that decreased and the swelling degree that increased with higher PVA content. The mechanical properties of membranes were also modified by the existence of PVA in the membranes composition, increasing the elongation capacity of these structures and decreasing the supported break stresses.

In 3D-scaffolds, not only the PVA ratio was evaluated, as well as the concentration of the casting solution and the freezing temperature used in the freeze-drying method. The scaffolds prepared with this technique are normally fragile and unstable in aqueous solution. To overcome this issue, it was applied a CO_2-assisted crosslinking process with glutaraldehyde comprising the study of different glutaraldehyde concentrations and operation times. SEM and mercury porosimetry results showed that the casting solution concentrations that were studied had no influence in the 3D-scaffolds porosity neither in the interconnectivity between pores. In addition, the presence of PVA content in these matrices and the temperature used in the freeze-drying process affected their morphology. In swelling tests the 3D-scaffolds proved

to be pH-sensitive and the best response was obtained for scaffolds crosslinked with 1% (v/v) of glutaraldehyde during 10 minutes.

Chitosan and PVA blended membranes and 3D-scaffolds were also tested for *in vitro* biodegradation and for cytotoxicity. The porous structures degraded along time in PBS solution containing lysozyme, with a higher degradation in the first days for matrices with more PVA content. In cytotoxicity tests, membranes were found to be non-cytotoxic, although a high content of PVA appeared to affect the cell attachment, morphology, proliferation and cell-cell contact. The results for crosslinked scaffolds showed no visible cytotoxic effects, except for high concentrations and high operation times where the cells response seemed to be affected. This reveals that the use of $scCO_2$ in the crosslinking treatment presents an advantage in the preparation of scaffolds, removing the remaining glutaraldehyde after the crosslinking process.

In conclusion, SCF technology allowed the preparation of sterile and ready-to-use devices, biodegradable and non-cytotoxic, with potential applications in tissue engineering and regenerative medicine, for example to support human stem cells proliferation and differentiation *in vitro* under controlled culture conditions.

5. References

[1] S. V. Madihally, H. W. T. Matthew, Porous chitosan scaffolds for tissue engineering, Biomaterials, 20 (1999) 1133-1142.

[2] G. Chen, T. Ushida, T. Tateishi, Scaffold design for tissue engineering, Macromol. Biosci., 2 (2002) 67-77.

[3] D. F. Stamatialis, B. J. Papenburg, M. Gironés, S. Saiful, S. N. M. Bettahalli, S. Schmitmeier, M. Wessling, Medical applications of membranes: Drug delivery, artificial organs and tissue engineering, Journal of Membrane Science, 308 (2008) 1-34.

[4] A. R. Sarasam, R. K. Krishnaswamy, S. V. Madihally, Blending Chitosan with Polycaprolactone: Effects on Physicochemical and Antibacterial Properties, Biomacromolecules, 7 (2006) 1131-1138.

[5] E. Chiellini, A. Corti, S. D'Antone, R. Solaro, Biodegradation of poly (vinyl alcohol) based materials, Prog. Polym. Sci., 28 (2003) 963-1014.

[6] S. Moscato, L. Mattii, D. D'Alessandro, M. G. Cascone, L. Lazzeri, L. P. Serino, A. Dolfi, N. Bernardini, Interaction of human gingival fibroblasts with PVA/gelatine sponges, Micron, 39 (2008) 569-579.

[7] J. J. J. A. Barry, S. N. Nazhat, F. R. A. J. Rose, A. H. Hainsworth, C. A. Scotchford, S. M. Howdle, Supercritical carbon dioxide foaming of elastomer/heterocyclic methacrylate blends as scaffolds for tissue engineering, J. Mater. Chem., 15 (2005) 4881-4888.

[8] R. Butler, C. M. Davies, I. Hopkinson, A. I. Cooper, Emulsion Templating using Supercritical Fluid Emulsions, Polymer Preprints, 43 (2002) 744-745.

[9] M. Temtem, T. Casimiro, A. Aguiar-Ricardo, Solvent power and depressurization rate effects in the formation of polysulfone membranes with CO_2-assisted phase inversion method, Journal of Membrane Science, 283 (2006) 244-252.

[10] M. Temtem, T. Casimiro, J. F. Mano, A. Aguiar-Ricardo, Preparation of membranes with polysulfone/polycaprolactone blends using a high pressure cell specially designed for a CO_2-assisted phase inversion, J. of Supercritical Fluids, 43 (2008) 542-548.

[11] K. Whang, C. H. Thomas, K. E. Healy, G. Nuber, A novel method to fabricate bioabsorbable scaffolds, Polymer, 36 (1995) 837-842.

[12] I. Pasquali, R. Bettini, F. Giordano, Supercritical fluid technologies: An innovative approach for manipulating the solid-state of pharmaceuticals, Advanced Drug Delivery Reviews, 60 (2008) 399-410.

[13] O. R. Davies, A. L. Lewis, M. J. Whitaker, H. Tai, K. M. Shakesheff, Applications of supercritical CO_2 in the fabrication of polymer systems for drug delivery and tissue engineering, Advanced Drug Delivery Reviews, 60 (2008) 373-387.

[14] C. Chen, C. Chang, Y. Chen, T. Lin, C. Su, S. Lee, Applications of Supercritical Fluid in Alloplastic Bone Graft: A Novel Method and *in Vitro* Tests, Ind. Eng. Chem. Res., 45 (2006) 3400-3405.

[15] F. Zhao, T. Ma, Perfusion bioreactor system for human mesenchymal stem cell tissue engineering: dynamic cell seeding and construct development, Biotechnol. Bioeng., 91 (2005) 482-493.

[16] L. Meinel, V. Karageorgiou, R. Fajardo, B. Snyder, V. Shinde-Patil, L. Zichner, D. Kaplan, R. Langer, G. Vunjak-Novakovic, Bone Tissue Engineering Using Human Mesenchymal Stem Cells: Effects of Scaffold Material and Medium Flow, Ann. Biomed. Eng., 32 (2004) 112-122.

[17] M. Temtem, L. M. C. Silva, P. Z. Andrade, F. Santos, C. L. Silva, J. M. S. Cabral, M. M. Abecasis, A. Aguiar-Ricardo, Supercritical CO_2 Generating Chitosan Devices with Controlled Morphology. Potential Application for Drug Delivery and Mesenchymal Stem Cell Culture. (accepted for publication in The Journal of Supercritical fluids).

[18] T. Freier, H. S. Koh, K. Kazazian, M. S. Shoichet, Controlling cell adhesion and degradation of chitosan films by N-acetylation, Biomaterials, 26 (2005) 5872-5878.

[19] C. Tangsadthakun, S. Kanokpanont, N. Sanchavanakit, R. Pichyangkura, T. Banaprasert, Y. Tabata and S. Damrongsakkul, The influence of molecular weight of chitosan on the physical and biological properties of collagen/chitosan scaffolds, J. Biomater. Sci. Polymer Edn, 18 (2007) 147-163.

[20] H. Hong, J. Wei, C. Liu, Development of asymmetric gradational-changed porous chitosan membrane for guided periodontal tissue regeneration, Composites: Part B, 38 (2007) 311-316.

[21] E. Reverchon, S. Cardea, E. Schiavo Rappo, Membranes Formation of a hydrosoluble biopolymer (PVA) using a supercritical CO_2–Expanded Liquid, J. of Supercritical Fluids, 45 (2008) 356-364.

[22] C. Chen, F. Wang, C. Mao, C. Yang, Studies of Chitosan. I. Preparation and Characterization of Chitosan/Poly(vinyl alcohol) Blend Films, Journal of Applied Polymer Science, 105 (2007) 1086-1092.

[23] E. Mangala, T. S. Kumar, S. Baskar, K. P. Rao, Development of chitosan/Poly (vinylalcohol) blend membranes as burn dressings, Trends Biomater. Artif. Organs., 17 (2003) 34-40.

[24] M. Cheng, J. Deng, F. Yang, Y. Gong, N. Zhao, X. Zhang, Study on physical properties and nerve cell affinity of composite films from chitosan and gelatin solutions, Biomaterials, 24 (2003) 2871-2880.

[25] A. Sarasam, S. V. Madihally, Characterization of chitosan–polycaprolactone blends for tissue engineering applications, Biomaterials, 26 (2005) 5500-5508.

[26] I. Adekogbe, A. Ghanem, Fabrication and characterization of DTBP-crosslinked chitosan scaffolds for skin tissue engineering, Biomaterials, 26 (2005) 7241-7250.

[27] S. Gunasekaran, T. Wang, C. Chai, Swelling of pH- Sensitive Chitosan–Poly(vinyl alcohol) Hydrogels, Journal of Applied Polymer Science, 102 (2006) 4665-4671.

[28] T. Koyano, N. Minoura, M. Nagura, K. Kobayashi, Attachment and growth of cultured fibroblast cells on PVA/chitosan-blended hydrogels, J. Biomed. Mater. Res., 39 (1998) 486-490.